PCCP

Formation and consumption of single-ring aromatic hydrocarbons and their precursors in premixed acetylene, ethylene and benzene flames†

Henning Richter* and Jack B. Howard

Department of Chemical Engineering, Massachusetts Institute of Technology, Cambridge, MA 02139-4307, USA. E-mail: richter@mit.edu

Received 6th November 2001, Accepted 12th March 2002
First published as an Advance Article on the web 30th April 2002

Kinetic modeling is becoming a powerful tool for the quantitative description of combustion processes covering different fuels and large ranges of temperature, pressure and equivalence ratio. In the present work, a reaction mechanism which was developed initially for benzene oxidation, and included the formation of polycyclic aromatic hydrocarbons was extended and tested for the combustion of acetylene and ethylene. Thermodynamic and kinetic property data were updated. If available, data were taken from the recent literature. In addition, density functional theory as well as *ab initio* computations on a CBS-Q and CBS-RAD level, partially published previously, were carried out. Quantum Rice–Ramsperger–Kassel analysis was conducted in order to determine pressure-dependent rate constants of chemically activated reactions. The model was developed and tested using species concentration profiles reported in the literature from molecular beam mass-spectrometry measurements in four unidimensional laminar premixed low-pressure ethylene, acetylene and benzene flames at equivalence ratios (ϕ) of 0.75 and 1.9 (C_2H_4), 2.4 (C_2H_2) and 1.8 (C_6H_6). Predictive capabilities of the model were found to be at least fair and often good to excellent for the consumption of the reactants, the formation of the main combustion products as well as the formation and depletion of major intermediates including radicals. Self-combination of propargyl (C_3H_3) followed by ring closure and rearrangement was the dominant benzene formation pathway in both rich acetylene and ethylene flames. In addition, reaction between vinylacetylene (C_4H_4) and vinyl radical (C_2H_3) contributed to benzene formation in the $\phi = 1.9$ ethylene flame. Propargyl formation and consumption pathways which involve reactions between acetylene, allene, propyne and singlet and triplet methylene were assessed. Significant overpredictions of phenoxy radicals indicate the necessity of further investigation of the pressure and temperature dependence and the product distribution of phenyl oxidation. The possible formation of benzoquinones, the ratio of the *ortho* and *para* isomers and their degradation pathways are of particular interest.

1. Introduction

Epidemiological studies have positively associated air pollution with lung cancer and cardiopulmonary disease[1–3] contributing an estimated 6% of total mortality, half of which was attributed to motorized traffic.[3] Fine particles formed by incomplete combustion, can be breathed more deeply into the lungs[4] and therefore are thought to pose a particularly great risk to health. At least part of the hazardous health effects of atmospheric aerosols might be related to their association with polycyclic aromatic hydrocarbons (PAH), some of which have been found to be mutagenic.[5] A molecular biological pathway linking one PAH—benzo[*a*]pyrene—to human lung cancer has been established.[6]

The role of PAH in flames as key intermediates in the inception and growth of soot which represents a major fraction of atmospheric aerosols is widely accepted[7,8] and the amounts of different PAH associated with different aerosol size fractions were measured.[9] The minimization of the formation of soot in combustion requires the control of chemical processes responsible for the growth of larger and larger PAH as well as their oxidation. Detailed kinetic modeling, the focus of the present work, provides deeper insight into these processes and allows the identification of optimized operating conditions.

In addition to the formation of undesired particulate matter, combustion of hydrocarbons has long been used for large-scale synthesis of carbon black[10] and recently it has been shown suitable for synthesis of fullerenes[11–15] and carbon nanotubes and other nanostructures.[16–22]

Optimization of combustion processes minimizing air pollution while maximizing energy release or yields of targeted materials requires detailed assessment of the controlling chemical reaction pathways. Combustion involves complex competition between species formation and destruction which, without oxidation, can lead to increasing large PAH and even soot particles.[7,8] The amounts of PAH and soot in the final combustion products depend on conditions such as temperature, pressure, fuel to oxygen ratio. Sooting tendencies of different fuel types increase from saturated aliphatics to unsaturated aliphatics and to aromatics.[7]

The present work identifies chemical reaction pathways responsible for fuel consumption, *e.g.*, bimolecular reactions leading to more reactive radicals, unimolecular decay, or both. Oxidation to CO, CO_2, H_2O and incompletely oxidized species such as formaldehyde (CH_2O) and formation of intermediates leading to PAH and soot were investigated. Oxidation and breakdown can occur at nearly any stage of combustion. For instance, consumption of initially formed PAH and their precursors can suppress their contribution to growth processes while acetylene formed in benzene destruction might play a significant role in the formation and growth of PAH and soot.

† Electronic supplementary information (ESI) available: Thermodynamic and kinetic property data. See http://www.rsc.org/suppdata/cp/b1/b110089k/

 DOI: 10.1039/b110089k

A kinetic model which allows qualitative and quantitative assessment of reactions responsible for fuel oxidation and formation of PAH and their precursors has been developed and applied to the combustion of acetylene, ethylene and benzene.

2. Method

Experimental structures of unidimensional premixed acetylene,[23,24] ethylene[25,26] and benzene[27] low pressure flames, consisting of temperature and mole fractions profiles of reactants, products and intermediates were taken from the literature. The comparison of experimental mole fractions to model predictions allowed assessment of predictive capabilities of the kinetic model. Main reaction pathways responsible for the formation and consumption of key species were identified after determination of the net rates of production, *i.e.*, the contribution, of individual reactions.

Acetylene, ethylene and benzene are major components of commonly used fuels, in addition acetylene and benzene are thought to play key roles in the formation of PAH and soot. For instance, the contribution of acetylene to PAH growth involves its sequential addition to PAH radicals *via* the hydrogen-abstraction–acetylene-addition mechanism.[28,29] In the case of non-aromatic fuels, the formation of the first aromatic ring, usually benzene, naphthalene or a derivative of these, is thought to be crucial for the ''kick-off'' of the growth process. Therefore, in this work, particular attention is paid to benzene formation from aliphatic species as well as its consumption by oxidation or subsequent PAH growth. Acetylene[23,24] and ethylene flames[25,26] are particularly valuable for the investigation of benzene formation while details of subsequent reaction pathways, *i.e.*, oxidation or PAH growth, can be assessed with benzene as the initial fuel.[27]

The experimental conditions of the four premixed unidimensional flat flames investigated here are given in Table 1. Mole fraction profiles of reactants, products and intermediate species were determined for all four flames by molecular beam sampling coupled to mass spectrometry (MBMS). Thermocouple measurements corrected for radiative heat loss gave temperatures along the axis above the burner. The ability to follow the evolution of radical concentrations makes MBMS valuable for studying elementary chemical processes in hydrocarbon combustion.[30]

Detailed kinetic models are widely used in quantitative studies of combustion processes. Improved computational power has permitted the development of increasingly complex reaction networks.[31] Experimental concentration profiles of stable and radical species measured in fuel-rich acetylene/oxygen/argon flames were compared with model predictions.[23,32] Routes leading to benzene have been suggested[32,33] and the formation of PAH described.[34] Recently, Lindstedt and Skevis[35] developed a detailed kinetic model including benzene formation and oxidation and compared model predictions to experimental data for six fuel-lean (normalized fuel/oxygen or equivalence ratio $\phi = 0.12$) to sooting ($\phi = 2.5$) laminar, premixed, low-pressure acetylene flames.

Kinetic schemes for fuel-rich ethylene combustion have been developed and compared to experimental flame structure data measured at atmospheric pressure.[36–38] Wang and Frenklach[39] studied the formation of PAH and their precursors and compared their model predictions to experimental results obtained by other authors for acetylene and ethylene combustion at different conditions.[23,24,28,40] The low pressure premixed acetylene flame of Westmoreland *et al.*,[23,24] was also investigated in the present work. In a recent study, Pope and Miller[41] assessed benzene formation pathways in three fuel-rich low-pressure premixed acetylene, ethylene and propene flames.

Several researchers have developed kinetic models for fuel-rich benzene combustion[42–44] and applied them to a premixed low-pressure benzene/oxygen/argon flame, also studied in this work, for which the structure was measured by Bittner and Howard[27] using MBMS. Recently, additional experimental data for this flame including concentration profiles of PAH radicals became available from nozzle beam sampling with radical scavenging and subsequent analysis by gas chromatography coupled to mass spectrometry (GC-MS).[45–47]

The availability of experimental data is crucial for the development of kinetic models. However, conclusions based on the comparison between model predictions and experimental flame structures should also take into account possible uncertainties in the experimental results. For instance, temperature measurements, particularly in nearly-sooting conditions, are not straight forward and the use of indirect calibration techniques such as the estimation of ionization cross sections can induce a significant uncertainty.

Kinetic model developed in present work

The kinetic network developed in the present work was initially based on the study of Shandross *et al.*[48] which focused mainly on benzene oxidation. The mechanism was subsequently extended to PAH up to coronene ($C_{24}H_{12}$) and C_{60} and C_{70} fullerenes.[49] Its predictions have been compared to experimental data in nearly sooting[27] and sooting[50] premixed benzene/oxygen/argon flames. Thermodymamic data have been revised using recent literature and density-functional theory (DFT) calculations followed by vibrational analysis.[47] The potential energy surfaces of reactions of acetylene with phenyl and 1-napththyl were explored by density-functional theory and high-pressure-limit rate constants were deduced *via* transition state theory. Pressure- and temperature-dependent rate constants which describe the formation of the different products of these chemically-activated reactions were determined by bimolecular QRRK (quantum Rice–Ramsperger–Kassel) analysis using the modified strong collision approach. Details of the techniques used in the present work for the determination of thermodynamic and kinetics properties were published recently.[51] In addition, density functional theory coupled with the use of isodesmic reactions and vibrational analysis served for the determination of thermodynamic properties of a large number of additional species included in the present mechanism. For some selected species *ab initio* calculation on a CBS-Q level were performed.[52] The complete set of standard heats of formation, entropies and heat capacities used in the present work is given in Table 2 (see Electronic Supplementary Information (ESI)†) and is available on-line.[53] In addition to the above-mentioned reactions of acetylene with phenyl and 1-naphthyl, presssure-dependence of other chemically activated reactions was taken into account and rate constants

Table 1 Parameters of flames investigated in the present work

Flame	Fuel	Equivalence ratio (ϕ)	Dilution/% of argon	Cold gas velocity/cm s^{-1}	Pressure/Torr	Ref.
I	Acetylene	2.4	5	50	20	23,24
II	Ethylene	0.75	56.91	62.5	30	25
III	Ethylene	1.9	50	62.5	20	26
IV	Benzene	1.8	30	50	20	27,46

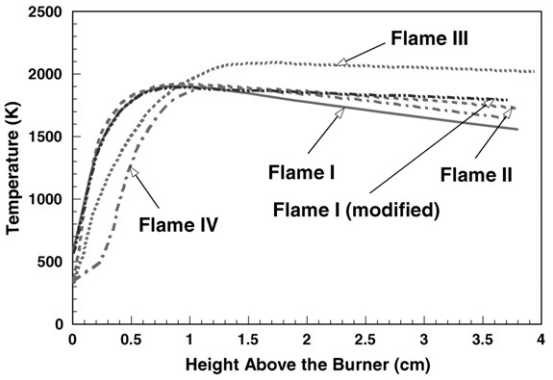

Fig. 1 Experimental temperature profiles used as input for kinetic modeling: —: Flame I: fuel-rich acetylene/oxygen/argon flame ($\phi = 2.4$, 5% argon, $v = 50$ cm s^{-1}, 20 Torr);[23,24] –·–: Flame I: increased temperature in the postflame zone (see text); ---: Flame II: fuel-lean ethylene/oxygen/argon flame ($\phi = 0.75$, 56.91% argon, $v = 62.5$ cm s^{-1}, 30 Torr);[25] ···: Flame III: fuel-rich ethylene/oxygen/argon flame ($\phi = 1.9$, 50.0% argon, $v = 62.5$ cm s^{-1}, 20 Torr);[26] –·–: Flame IV: nearly sooting benzene/oxygen/argon flame ($\phi = 1.8$, 30% argon, $v = 50$ cm s^{-1}, 20 Torr).[27]

for the low-pressure conditions pertinent to the present work were determined by QRRK computations,[54,55] if no suitable literature values were available. The mechanism developed in the present study is given in Table 3† as well as on-line[53] and includes the sources of all kinetic data.

Testing of the model. All model calculations were performed with the PREMIX flame code, a part of the CHEMKIN software package.[56–58] Experimental temperature profiles, shown in Fig. 1, were used for all computations. In addition to the original experimental temperature profile of the fuel-rich acetylene flame[23,24] (Flame I), a profile modified in the postflame zone is given and was used for the model predictions of this flame presented here. An increase of the temperature in the postflame zone was based on inconsistencies in model predictions of benzene and phenyl (see below) and possible soot deposition on the thermocouple during the measurement. Comparisons of model predictions with experimental mole fraction profiles measured in the four investigated flames (Table 1) are discussed below. Major pathways of fuel consumption and oxidation as well as of the formation of PAH precursors were identified subsequent to the computation of net rates of production of the species of interest using the postprocessor included in the CHEMKIN collection.[58] Area expansion of the unidimensional flames was taken into account in all computations using the corresponding expressions given in the literature.[23,25–27] In the case of the lean[25] and rich[26] ethylene flames, area expansion was rescaled in order to be equal to unity at the burner surface.

3. Results

The initial consumption steps of the fuels acetylene, ethylene and benzene, subsequent reaction steps leading to total oxidation of the fuel, *i.e.*, to CO, CO_2 and H_2O, and competing pathways responsible for PAH growth are discussed below.

The analysis of the rates production shows that the reactions responsible for the consumption of the initial fuel, *i.e.*, in the present work acetylene, ethylene and benzene, depend significantly on the conditions of the combustion process, in particular temperature and pressure. Many reactions are at, or close to, their equilibrium and reversibility was assumed for all reactions included in the mechanism. Many PAH formation reactions are tightly balanced,[34,39,47] so that their contribution to consumption or formation of a species at a given position in a flame depends on the local temperature and concentrations of the reactants and products. Pressure has a significant impact on reactions with different numbers of molecules of reactants and products due to their pressure-depending equilibrium constants and on unimolecular reactions whose rate coefficients increase with pressure.

Consumption of initial fuel: Acetylene

The analysis of the intial steps of acetylene consumption is based on the modeling of the premixed low-pressure acetylene/oxygen/argon flame ($\phi = 2.4$, 5% argon, cold gas velocity $v = 50$ cm s^{-1}, 20 Torr) studied by Westmoreland *et al.*[23,24] using MBMS (Flame I). Predicted mole fraction profiles of acetylene and oxygen are compared to experimental data in Fig. 2. Key features such as a nearly constant acetylene concentrations beyond 1.5 cm above the burner and the nearly complete oxygen depletion in the postflame zone are predicted correctly but the predicted consumptions of acetylene and oxygen are slower than the data show. The acetylene mole fraction remaining in the postflame zone is overpredicted by about 25%. Possible explanations might be uncertainties in the temperature profile used in the model calculation or possible perturbation of the flame by the sampling probe. Temperature measurement in near sooting or sooting flames is particularly challenging, *e.g.*, due to possible deposits on the thermocouple which can lead to a significant decrease (up to several hundred K) of the reading. The effect of temperature on the predicted acetylene profile was tested. For instance, an increase of the maximum temperature (at 0.8 cm from the burner) profile by 200 K to 2100 K and the maintain of this temperature in the postflame zone led to a good agreement of the model predictions with the experimental acetylene mole fractions in the burnt gas mixture (not shown). However, the latter temperature profile is hypothetical and such large deviations from measured data must be considered as unlikely.

Also, acetylene mole fractions predicted in the postflame zone were found to be extremely sensitive to the thermodynamic properties. A significant improvement was also achieved by using the thermodynamic properties of acetylene suggested by Burcat and McBride[59] instead of the NIST recommendation for the heat of formation ($\Delta H_f^\circ = 54.19$ kcal mol^{-1})[60] in conjunction with the entropy and heat capacities determined by means of density functional theory.[47,51] The differences between the thermodynamic values suggested by Burcat and McBride[59] and those used in our laboratory[47,51] are 0.16 kcal mol^{-1} for the heat of formation (ΔH_f°) and −0.64, −0.77, −0.46, −0.31, −0.26, −0.16, 0.02, 0.20 cal mol^{-1} K^{-1} for the entropy (S_f°) and heat capacities at 300, 400, 500, 600, 800, 1000, 1500 K, respectively. These discrepancies are close to

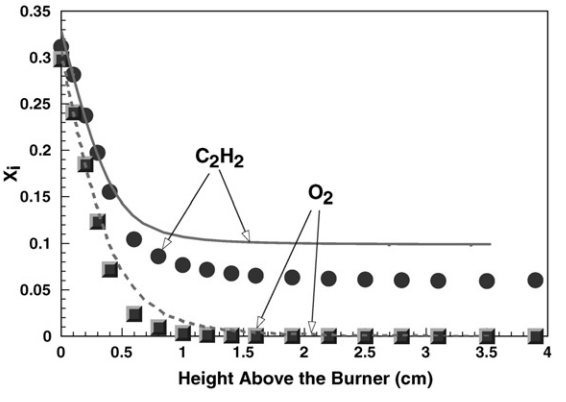

Fig. 2 Comparison between experimental mole fraction profiles[23,24] and model predictions in a fuel-rich acetylene/oxygen/argon flame ($\phi = 2.4$, 5% argon, $v = 50$ cm s^{-1}, 20 Torr); C_2H_2: ● (experiment), — (prediction); O_2: ■ (experiment), --- (prediction).

the limits of uncertainty imposed by the use of 14-parameter fits ("NASA polynomia") for heats of formation, entropies and heat capacities.[61] The significant impact of these discrepancies on the model prediction of acetylene emphasizes the extreme importance of reliable thermodynamic data. In the present work, the heat of formation recommended by NIST[60] and the entropy and heat capacities determined by means of density functional theory followed by vibrational analysis[47,51] were used in order to maintain consistency of the thermodynamic data set. Entropy and heat capacities of acetylene are also included in the NIST database;[60] the recommended values are very similar to those used in present work. In addition, the impact of the discussed variation of thermodynamic data of acetylene on mole fraction profiles predicted by the kinetic model has been assessed for other species such as HCO, only minor effects were observed.

The net consumption rate of acetylene, *i.e.*, the sum of the contributions of all reactions, increases rapidly close to the burner and exhibits a sharp maximum at about 0.4 cm above the burner. The net rate then decreases and reaches essentially zero at about 2 cm from the burner. Simultaneously, the contributions of all individual reactions also approach zero. Therefore, the constant concentration of acetylene in the post-flame zone is not due to a balancing of acetylene formation and destruction pathways but to a drastic slow down of all reactions involving acetylene beyond the reaction zone. The most important single reaction consuming acetylene is

$$C_2H_2 + O \rightleftharpoons HCCO + H. \quad (211)$$

The ketone radical HCCO is subsequently oxidized to CO, the most important consumption reactions being

$$HCCO + H \rightleftharpoons {}^1CH_2 + CO \quad (165)$$

and

$$HCCO + O_2 \rightleftharpoons 2CO + OH. \quad (169)$$

Other significant acetylene consumption pathways are, in order of decreasing importance, oxidation to $^3CH_2$ and CO *via* reaction (210)† and its reaction with $^1CH_2$ to propargyl (C_3H_3) and H (reaction (321)). Both singlet and triplet methylene ($^1CH_2$ and $^3CH_2$) are easily oxidized to formaldehyde (CH_2O), CO and CO_2. Propargyl plays a key role in benzene formation *via* its recombination followed by rearrangement[33] and will be discussed later in more detail.

Ethylene (C_2H_4) is the second most abundant hydrocarbon, next to acetylene, in the rich acetylene flame studied here.[23,24] Analysis of the rates of production showed that sequential hydrogen addition to acetylene does not contribute significantly to ethylene formation. The major formation pathways were found to be reactions

$$CH_3 + CH_3 \rightleftharpoons C_2H_4 + H_2, \quad (111)$$

$$^3CH_2 + CH_3 \rightleftharpoons C_2H_4 + H \quad (235)$$

as well as unimolecular decay of n- and i-C_3H_7 (reactions (436) and (437)†). Ethylene consumption in this acetylene flame occurs mainly by hydrogen abstraction with H and OH forming vinyl (C_2H_3) (reactions (232) and (244)†).

Assessment of predictive capability. In the critical testing of kinetic models for combustion chemistry by comparison of model predicted species concentration profiles against experimental data, profiles of radicals provide a more sensitive and meaningful test than do the profiles of stable species. Radicals are key intermediates in flame chemistry and the ability to predict their concentrations at different stages of combustion is essential for the accurate prediction of the flame properties and behavior of interest. Compared to concentrations of stable species, the concentrations of radicals are more difficult to measure and are known with larger uncertainty. Accurate modeling of radical formation and consumption is challenging because of the enhanced sensitivity to thermodynamic and kinetic properties and to the temperature profile used. Mole fraction profiles of H, OH, CH_3, HCO, CO and CO_2 computed for Flame I are compared to experimental data in Figs. 3 and 4. Abstraction of hydrogen atoms by H and OH is a key step in the formation of a large range of hydrocarbon radicals while HCO is a key intermediate in the oxidation leading ultimately to CO and CO_2. Methyl is the most abundant radical identified in the rich acetylene flame studied here.[23,24] Encouraging agreement between model predictions and experimental mole fraction profiles can be seen in Figs. 3 and 4 for OH, HCO and CH_3 but a significant overprediction of H, especially in the reaction zone, is observed.

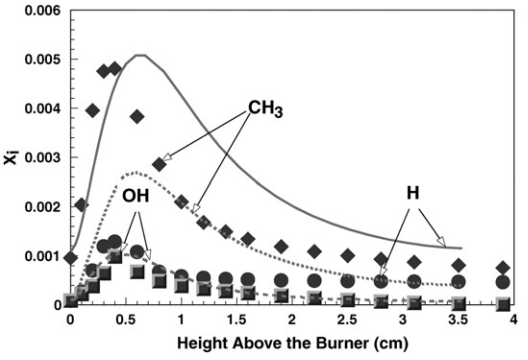

Fig. 3 Comparison between experimental mole fraction profiles[23,24] and model predictions in a fuel-rich acetylene/oxygen/argon flame ($\phi = 2.4$, 5% argon, $v = 50$ cm s^{-1}, 20 Torr); H: ● (experiment), — (prediction); OH: ■ (experiment), --- (prediction); CH_3: ◆ (experiment), ··· (prediction).

Consumption of initial fuel: Ethylene

A fuel-lean[25] and a fuel-rich[26] premixed low-pressure ethylene/oxygen/argon flame (Flames II and III, respectively; Table 1) were studied and used for the determination of ethylene consumption steps. The comparison of model predictions with experimental data for both flames allowed the reliability of the present model to be assessed over a large range of equivalence ratios. A major difference between these two flames is the fast and nearly complete conversion of ethylene to CO, CO_2 and H_2O in the fuel-lean flame. Computed and experimental mole fraction profiles of ethylene and oxygen in Flame II are given in Fig. 5 while profiles for the stable products, *i.e.*,

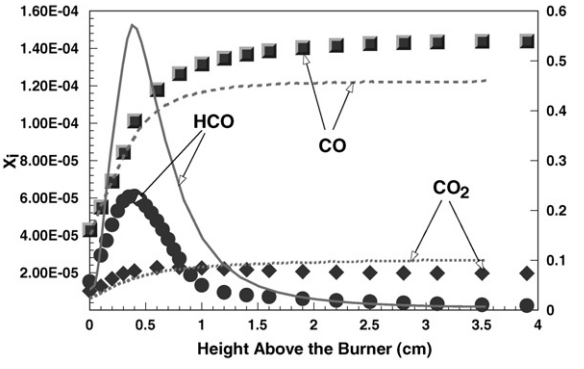

Fig. 4 Comparison between experimental mole fraction profiles[23,24] and model predictions in a fuel-rich acetylene/oxygen/argon flame ($\phi = 2.4$, 5% argon, $v = 50$ cm s^{-1}, 20 Torr); HCO: ● (experiment, left scale), — (prediction, left scale); CO: ■ (experiment, right scale), --- (prediction, right scale); CO_2: ◆ (experiment, right scale), ··· (predicght scale).

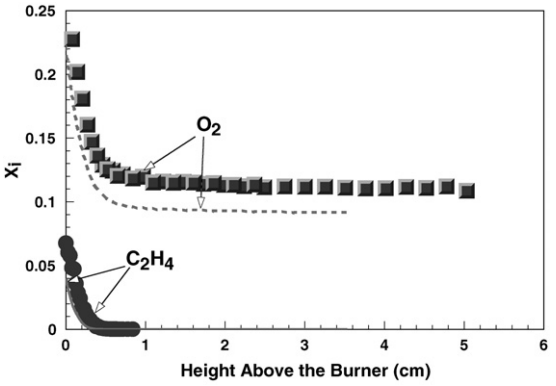

Fig. 5 Comparison between experimental mole fraction profiles[25] and model predictions in a fuel-lean ethylene/oxygen/argon flame ($\phi = 0.75$, 56.91% argon, $v = 62.5$ cm s^{-1}, 30 Torr); ethylene (C_2H_4): ● (experiment), — (prediction); O_2: ■ (experiment), --- (prediction).

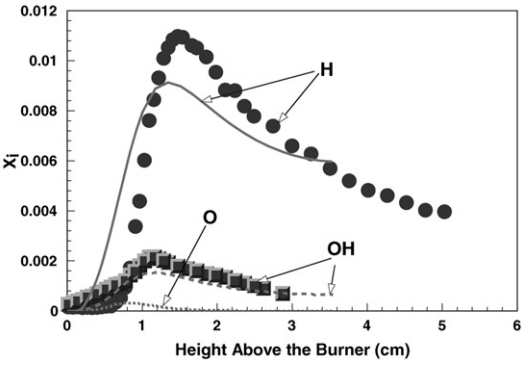

Fig. 7 Comparison between experimental mole fraction profiles[26] and model predictions in a fuel-rich ethylene/oxygen/argon flame ($\phi = 1.9$, 50.0% argon, $v = 62.5$ cm s^{-1}, 20 Torr); H: ● (experiment), — (prediction); OH: ■ (experiment), --- (prediction); O: ··· (prediction).

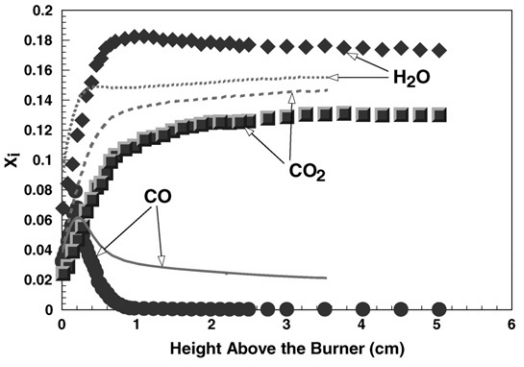

Fig. 6 Comparison between experimental mole fraction profiles[25] and model predictions in a fuel-lean ethylene/oxygen/argon flame ($\phi = 0.75$, 56.91% argon, $v = 62.5$ cm s^{-1}, 30 Torr); CO: ● (experiment), — (prediction); CO_2: ■ (experiment), --- (prediction); H_2O: ◆ (experiment), ··· (prediction).

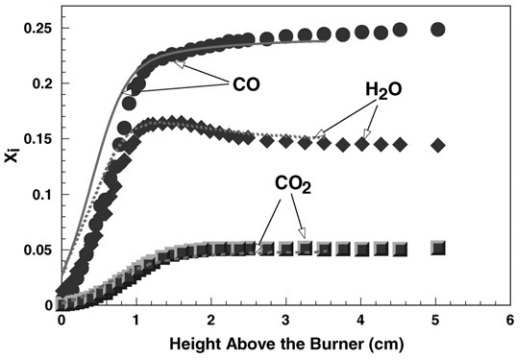

Fig. 8 Comparison between experimental mole fraction profiles[26] and model predictions in a fuel-rich ethylene/oxygen/argon flame ($\phi = 1.9$, 50.0% argon, $v = 62.5$ cm s^{-1}, 20 Torr); CO: ● (experiment), — (prediction); CO_2: ■ (experiment), --- (prediction); H_2O: ◆ (experiment), ··· (prediction).

CO, CO_2 and H_2O are shown in Fig. 6. The insufficient depletion of CO predicted in the postflame zone is probably related to a more than two-fold overpredition of hydrogen radicals, in particular far from the burner, which shifts the equilibrium of reaction

$$CO + OH \rightleftharpoons CO_2 + H \qquad (39)$$

to the left and increases the CO concentrations. Another possible source of error might be an overestimation in the difficult flame temperature measurement, discussed above. The use of overestimated temperatures in the model computation for Flame II could also explain the slightly too fast consumption of ethylene and oxygen (Fig. 5), the overprediction of OH (by up to 50%) and the ~20% underprediction of H_2O (Fig. 6).

Good to very good agreements of model predictions with the corresponding experimental data were achieved in Flame III, the fuel-rich ethylene flame.[26] Experimental and predicted mole fraction profiles are shown in Figs. 7 and 8 for H, OH, H_2O, CO and CO_2. In addition, the model prediction for O-atoms is added in Fig. 7; experimental data for this species in this flame are not available, probably due to its low concentration and mass overlap with methane in mass spectrometry.

The identity of the main ethylene consumption pathways depends strongly on the local flame conditions and therefore on the height above the burner and the equivalence ratio. Reaction of ethylene with hydrogen radicals can occur *via* two different channels: (i) hydrogen addition yielding ethyl radicals and (ii) hydrogen abstraction giving vinyl radicals (C_2H_3) and H_2. Both reactions have been studied extensively and a rate constant suggested by Tsang and Hampson[62] was used for the channel leading to ethyl radicals, *i.e.*,

$$C_2H_4 + H \rightleftharpoons C_2H_5 \qquad (233)$$

while the kinetic data derived by Knyazev *et al.*[63] for

$$C_2H_4 + H \rightleftharpoons C_2H_3 + H_2, \qquad (232)$$

based on experimental and *ab initio* computational results, were used for hydrogen abstraction. Comparison of the main reaction pathways responsible for ethylene consumption in a fuel-lean and a fuel-rich flame reveals significant differences. In the rich ethylene flame, the reaction zone extends to ~1.5 cm above the burner while in the lean flame the net rate of production of ethylene and the contribution of individual reactions reach essentially zero at about 0.5 cm from the burner.

In the lean flame, hydrogen addition leading to ethyl radicals (reaction (233)) is the dominant consumption pathway close to the burner and is responsible for a pronounced local minimum of the net rate of production of ethylene at a height above the burner of about 0.1 cm (Fig. 9). At increasing heights above the burner, the contribution of reaction (233) to ethylene consumption decreases dramatically and becomes an ethylene forming pathway with a local maximum of its net rate of formation at about 0.14 cm. This behaviour can be explained by the relatively strong temperature dependence of the rate constant of hydrogen abstraction (reaction (232)) favoring ethyl formation at low temperatures. Reactions of ethylene with H, O and OH radicals, *i.e.*, reactions (233), (243)–(245) and (284)† result in an unambiguous net consump-

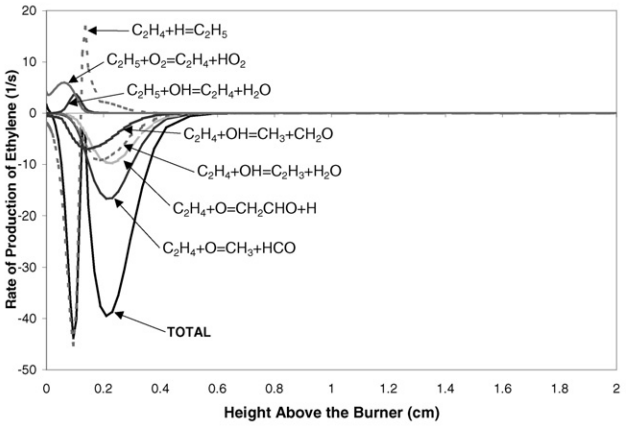

Fig. 9 Rates of production of ethylene computed from model predictions in a fuel-lean ethylene/oxygen/argon flame ($\phi = 0.75$, 56.91% argon, $v = 62.5$ cm s^{-1}, 30 Torr)[25] —: total; —: $C_2H_5 + O_2 \rightleftharpoons C_2H_4 + HO_2$; ···: $C_2H_4 + H \rightleftharpoons C_2H_5$; —: $C_2H_5 + OH \rightleftharpoons C_2H_4 + H_2O$; —: $C_2H_4 + O \rightleftharpoons CH_3 + HCO$; ---: $C_2H_4 + O \rightleftharpoons CH_2CHO + H$; ···: $C_2H_4 + OH \rightleftharpoons C_2H_3 + H_2O$; ---: $C_2H_4 + OH \rightleftharpoons CH_3 + CH_2O$.

tion of ethylene as shown in Fig. 9. The relative contributions of the different reactions depend on the relative concentrations of H, O and OH radicals as well as on the local, temperature-dependent, rate constants. For instance, in the lean flame, hydrogen abstraction by H radicals (reaction (232)) contributes about 20 times less to ethylene consumption than the corresponding reaction with OH. However, under fuel-rich conditions reaction (232) is the dominant pathway, reflecting the large concentration of H relative to that of OH.

Also in the rich flame, formation of ethyl radicals *via* reaction (233) leads to a local maximum of the ethylene consumption rate close to the burner but in contrast to the lean case the reverse reaction forms only insignificant amounts of ethylene at higher heights above the burner. Vinyl formation *via* reactions (232) and

$$C_2H_4 + OH \rightleftharpoons C_2H_3 + H_2O \qquad (244)$$

is the dominant ethylene consumption channel. In addition, ethylene oxidation by oxygen radicals, *i.e.*, *via* reactions

$$C_2H_4 + O \rightleftharpoons CH_3 + CHO \qquad (243)$$

and

$$C_2H_4 + O \rightleftharpoons CH_2CHO + H, \qquad (284)$$

contributes significantly to its depletion. Another ethylene consumption pathway, identified by analysis of the rates of production, is its reaction with methine (CH) leading to allene (H_2CCCH_2) and hydrogen radicals (reaction (358)†). The corresponding rate constant suitable for low-pressure conditions was determined in the present work by a QRRK analysis[54,55] using the measurement of Thiesemann *et al.*[64] for the entrance channel and the expression derived by Tsang and Walker[65] for the unimolecular loss of hydrogen from the C_3H_5 adduct.

Vinyl. Vinyl (C_2H_3) is the major acetylene precursor in both ethylene flames. Hydrogen abstraction from ethylene by H and OH (reactions (232) and (244)) is its dominant formation route in all the flames, including those of acetylene and benzene, investigated in this work. Comparison of the predicted vinyl mole fraction profile with experimental data (Fig. 10) shows good agreement of the peak value in the lean ethylene flame (Flame II). However, the predicted breath of the profile is only about 0.4 cm compared to ~0.7 cm for the experimental one. Shape and peak location are in good agreement for all other flames (Flames I, III and IV) but a three to five-fold overprediction of the peak value is observed. The most important vinyl consumption reactions are its oxidation with molecular oxygen *via* reaction

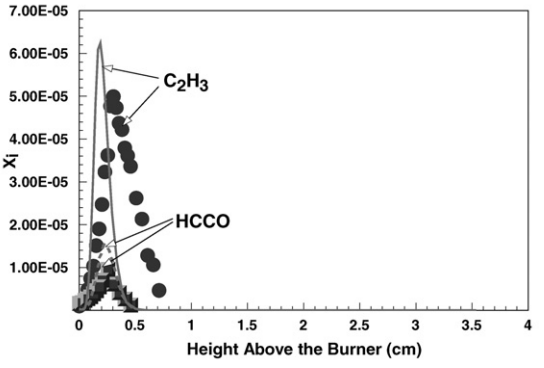

Fig. 10 Comparison between experimental mole fraction profiles[25] and model predictions in a fuel-lean ethylene/oxygen/argon flame ($\phi = 0.75$, 56.91% argon, $v = 62.5$ cm s^{-1}, 30 Torr); vinyl (C_2H_3): ● (experiment), — (prediction); ketenyl (HCCO): ■ (experiment), --- (prediction).

$$C_2H_3 + O_2 \rightleftharpoons CH_2O + HCO \qquad (224)$$

and unimolecular hydrogen-loss leading to acetylene, *i.e.*, reaction

$$C_2H_3 \rightleftharpoons C_2H_2 + H. \qquad (213)$$

Pressure and temperature dependence of reaction (213) have been assessed by Knyazev and Slagle[66] based on experimental data and master equation modeling. Their suggested rate constant was confirmed in the present work by means of a QRRK analysis of the reverse reaction and is used in the kinetic model developed here. Also, hydrogen abstraction by H, O, O_2, OH and CH_3 (reactions (214), (216), (225), (226) and (229)†) contributes significantly to vinyl consumption and acetylene formation. Other non-negligible vinyl-consumption pathways involve its oxidation by O and OH:

$$C_2H_3 + O \rightleftharpoons CH_2CO + H, \qquad (215)$$

$$C_2H_3 + O \rightleftharpoons CO + CH_3, \qquad (217)$$

$$C_2H_3 + O \rightleftharpoons HCO + {}^1CH_2 \qquad (223)$$

and

$$C_2H_3 + OH \rightleftharpoons CH_3CHO. \qquad (301)$$

Acetylene. Acetylene formation and consumption are well predicted in the rich ethylene flame (Fig. 11) while the peak mole fraction is by ~threefold underpredicted in the lean ethylene flame. The analysis of the rates of production showed the above discussed vinyl consumption reactions to be the major acetylene formation pathways. In the lean flame, acetylene is completely depleted beyond about 0.8 cm from the burner. In the rich flame a significant mole fraction of about 1% remains in the postflame zone. The major acetylene consumption pathway in both flames is its oxidation with O to the ketenyl radical HCCO: (reaction (211)). Subsequently, HCCO is consumed by reaction with H and O radicals: reactions (165) and

$$HCCO + O \rightleftharpoons 2CO + H. \qquad (166)$$

Species corresponding to the molecular mass of HCCO were identified in both lean and rich ethylene flames. Comparison of the model predictions with the experimental mole fraction profiles gave an excellent agreement in the lean flame (Fig. 10) but an approximately four-fold overprediction was observed in the rich ethylene flame. Reaction pathways identi-

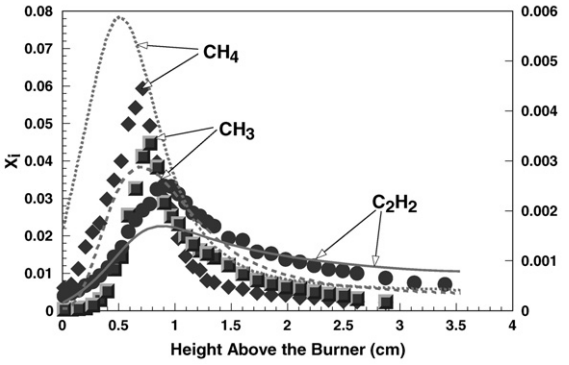

Fig. 11 Comparison between experimental mole fraction profiles[26] and model predictions in a fuel-rich ethylene/oxygen/argon flame ($\phi = 1.9$, 50.0% argon, $v = 62.5$ cm s^{-1}, 20 Torr); C_2H_2: ● (experiment, left scale), — (prediction, left scale); CH_3: ■ (experiment, right scale), --- (prediction, right scale); CH_4: ◆ (experiment, right scale), ··· (prediction, right scale).

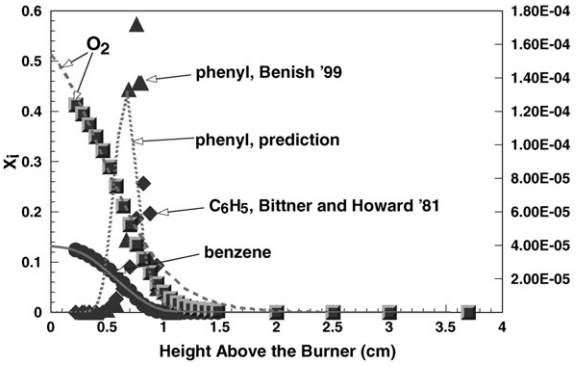

Fig. 12 Comparison between experimental mole fraction profiles and model predictions in a nearly sooting benzene/oxygen/argon flame ($\phi = 1.8$, 30% argon, $v = 50$ cm s^{-1}, 20 Torr); benzene: ● (experiment,[27] left scale), — (prediction, left scale); O_2: ■ (experiment,[27] left scale), --- (prediction, left scale); C_6H_5: ◆ (experiment,[27] right scale); phenyl: ▲ (experiment,[46] right scale), ··· (prediction, right scale).

fied as being responsible for acetylene consumption are qualitatively, and in a large extent quantitatively, identical to those discussed above for a premixed acetylene/oxygen/argon flame.[23,24] The absence of a contribution of reaction

$$^1CH_2 + C_2H_2 \rightleftharpoons C_3H_3 + H \qquad (321)$$

to acetylene consumption in the fuel-lean ethylene flame is consistent with propargyl (C_3H_3) being a precursor of benzene which is only observed in trace quantities in this flame.

Methyl. Methyl is usually the most abundant hydrocarbon radical in flames and it has been suggested to contribute to PAH formation.[27] In the present work, at least satisfactory agreement between model predictions and experimental data were achieved for methyl and methane in the rich ethylene flame (Fig. 11) and in the benzene flame. However, the model exhibited insufficient methane depletion in the postflame zone of the rich acetylene flame and a significant underprediction for both methyl and methane in the lean ethylene flame.

Consumption of initial fuel: Benzene

Benzene consumption by oxidative degradation and PAH growth reactions was investigated here by kinetic modeling of a premixed low-pressure nearly sooting benzene/oxygen/argon flame[27,46] (Flame IV) for which a large body of experimental data including mole fraction profiles of radical intermediates is available. The use of benzene flame data in kinetic modeling facilitates the study of major benzene consumption reactions because the concentrations of the involved species are considerably higher than in flames of other fuels.

The analysis of the net rates of benzene consumption in the premixed benzene shows the importance of the formation of relatively unstable benzene derivatives in a first reaction step and which are consumed subsequently. H, O and OH radicals are crucial for this initial activation and the relative contribution of the different pathways is expected to depend significantly on the mole fractions of these species. The model predictions for benzene and O_2 agree well with the experimental data[27] up to a distance of about 0.8 cm from the burner surface while farther from the burner the predicted benzene and O_2 depletion is slightly slower than in the experimental profiles (Fig. 12). However, consistent with the experiments, both benzene and oxygen are entirely consumed in the postflame zone. Predictions of mole fraction profiles of H, O and OH are given in Fig. 13 and exhibit excellent agreement with experimental data. Experimental data for atomic oxygen are only available in the late part of the reaction zone and the postflame zone

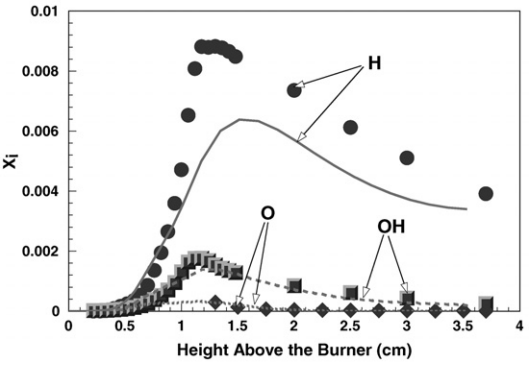

Fig. 13 Comparison between experimental mole fraction profiles[27] and model predictions in a nearly sooting benzene/oxygen/argon flame ($\phi = 1.8$, 30% argon, $v = 50$ cm s^{-1}, 20 Torr); H: ● (experiment), — (prediction); OH: ■ (experiment), --- (prediction); O: ◆ (experiment), ··· (prediction).

due to the overlap with methane in mass spectrometric detection.

Using the rate constant determined experimentally by Madronich and Felder[67] over the temperature range from 790 to 1410 K at subatmospheric pressure, hydrogen abstraction *via*

$$C_6H_6 + OH \rightleftharpoons C_6H_5 + H_2O \qquad (647)$$

was found to be the most important benzene consumption pathway close to the burner in the benzene flame studied here. Madronich and Felder[67] also showed that formation of phenol and hydrogen radicals did not contribute significantly to the overall reaction rate of $C_6H_6 + OH$. Nevertheless, the possibility of this pathway should not be entirely excluded at other conditions than those investigated by these authors, *e.g.*, high pressure. Therefore, reaction (652)

$$C_6H_6 + OH \rightleftharpoons C_6H_5OH + H \qquad (652)$$

has been included in the present model. Its rate constant was estimated at conditions relevant for this work in a QRRK computation[55] using input parameters similar to those suggested by Shandross *et al.*[48] Nevertheless, reaction (652) does not contribute significantly to benzene consumption. Reaction of benzene with O atoms to give phenoxy and H, *i.e.*,

$$C_6H_6 + O \rightleftharpoons C_6H_5O + H, \qquad (646)$$

is another important consumption pathway up to ~0.7 cm from the burner, *i.e.*, nearly simultaneously with reaction

(647). Ko *et al.*[68] investigated $C_6H_6 + O$ experimentally and suggested a rate constant over a temperature range from 300 to 1450 K which was used here. Ko *et al.*[68] also showed evidence that the O atom addition mechanism, *i.e.*, formation of $C_6H_5O + H$, dominated under the conditions of their study. Nevertheless, the possibility of a more important contribution of hydrogen abstraction *via* reaction (645),

$$C_6H_6 + O \rightleftharpoons C_6H_5 + OH \quad (645)$$

under low-pressure conditions can not be excluded taking into account that Ko *et al.*[68] collected all experimental data at pressures of not less than 240 mbar. Overestimation of phenoxy formation *via* reaction (646) at low pressure might be a possible explanation for the overprediction of this species in a premixed 22 Torr $H_2/O_2/Ar$ flame seeded with benzene.[48] The contribution of hydrogen abstraction with H atoms, *i.e.*,

$$C_6H_6 + H \rightleftharpoons C_6H_5 + H_2, \quad (644)$$

was shown to be similar to that of hydrogen abstraction with OH but was shifted by ~2 mm towards the postflame zone. The kinetic data used in the present work for reaction (644), and all similiar hydrogen abstraction reactions from PAH, have been deduced from the $C_6H_5 + H_2$ rate constant computed by Mebel *et al.*,[69] using the thermodynamic properties given in Table 2.† The resulting rate constant is in excellent agreement with the high temperature data determined in a shock tube study by Kiefer *et al.*,[70] *i.e.*, $2.5 \times 10^{14} \exp(-16\,000\ 000\ \text{cal}/RT)\ \text{cm}^3\ \text{mol}^{-1}\ \text{s}^{-1}$.

At the end of the reaction zone, unimolecular decay of benzene to propargyl (C_3H_3) *via* the reverse of

$$C_3H_3 + C_3H_3 \rightleftharpoons C_6H_6, \quad (638)$$

is the most important benzene consumption reaction. Its rate is maximum at ~1 cm above the burner. Propargyl recombination has been discussed as an important if not dominant route[33] for the formation of the first aromatic ring. Phenyl + H as well as benzene (and fulvene) have been suggested as possible products. In a recent shock tube study of pyrolytic reactions of propargyl radicals,[71] linear and/or aromatic C_6H_6 species were identified as main products while the formation rate of $C_6H_5 + H$ was less than 10% of the total rate. Benzene depletion by unimolecular decomposition to propargyl is consistent with these observations, but quantitative assessment of its contribution is not yet feasible due to the lack of a reliable pressure-dependent rate constant.

Benzene consumption pathways identified by analysis of benzene net production rates in the rich acetylene (Flame I) are similar to the findings from the benzene flame. Hydrogen abstraction *via* reaction (647) is dominant, due to its low activation energy, up to ~0.4 cm above the burner while reaction (644) becomes dominant farther from the burner. Reaction with OH to give phenol, *i.e.*, reaction (652), does not contribute significantly to benzene depletion while the reverse reaction even leads to benzene formation close to the burner. Benzene formation in the acetylene flame results mainly from propargyl recombination. However, the reverse reaction is a minor consumption pathway at the end of the reaction zone with a maximum rate at ~6–7 mm above the burner. Details of benzene formation chemistry in both acetylene and ethylene flames is discussed below.

The analysis of benzene net production rates showed that phenyl and to some extent phenoxy radicals are key intermediates in benzene depletion. The chemistry of formation and subsequently depletion of phenoxy and phenol is discussed below.

Phenyl: A key intermediate in benzene depletion

Phenyl represents a bifurcation between further oxidation, *i.e.*, decay to smaller species and growth to PAH. The complexity of its chemistry has proven to be challenging to model accurately.[42–44,48,49]

The contributions of individual reactions to the net phenyl production rate in the premixed benzene flame show that phenyl is formed nearly entirely from benzene *via* the hydrogen abstraction reactions (647) and (644), discussed above. The reverse of unimolecular hydrogen loss from phenyl to give benzyne,

$$C_6H_5 \rightleftharpoons \text{benzyne} + H, \quad (636)$$

is a minor phenyl formation pathway below ~0.65 cm above the burner and beyond 1.1 cm while the contribution of this reaction to phenyl consumption exhibits a maxium at ~0.8 cm. Unimolecular decay of phenyl was studied extensively by Madden *et al.*[72] in an *ab initio* MO study followed by a RRKM treatment. Their rate constants for the formation of benzyne and linear C_6H_4 (C_6H_4, 1,5-hexadiyn-3-ene) were used in the present work. Hydrogen loss to give linear C_6H_4, *i.e.*,

$$C_6H_5 \rightleftharpoons C_6H_4 + H, \quad (637)$$

was found to be a major phenyl consumption pathway with a maxium at ~0.85 cm from the burner. Phenyl isomerization to 1,3-dien-6-yne radicals, *i.e.*, ring opening,

$$C_6H_5(L) \rightleftharpoons C_6H_5, \quad (631)$$

also identified on the potential energy surface by Madden *et al.*,[72] is the most important phenyl consumption reaction in the later part of the reaction zone, *i.e.*, between 0.8 and 1.3 cm from the burner. Its production rates show that linear C_6H_5 (1,3-dien-6-yne radicals) decays quickly to linear C_6H_4 (reaction (624)†). The peak mole fraction of linear C_6H_5 was predicted to be more than three orders of magnitude smaller than that of phenyl. Model predictions compared with the C_6H_4 mole fraction profile of species measured by MBMS[27] show good agreement in shape and location but the peak value is overpredicted ~2.5 fold if the C_6H_4 is linear or ~threefold if it is benzyne. The predicted 1,3,5-hexatriyne (triacetylene, C_6H_2) peak is ~80% higher than the corresponding experimental value.[27] Analysis of production rates shows 1,3,5-hexatriyne to be formed by sequential hydrogen release and abstraction beginning with linear C_6H_4 while

$$C_4H_2 + C_2H \rightleftharpoons C_6H_2 + H \quad (613)$$

was identified as major consumption pathway. A similar analysis in the acetylene flame, shows reaction (613) to be a major 1,3,5-hexatriyne formation pathway while sequential hydrogen release/abstraction from linear C_6H_4 is also significant.

Other, minor, phenyl consumption pathways in the later part of the reaction zone of the benzene flame are the reverse of reactions

$$\text{n-}C_4H_3 + C_2H_2 \rightleftharpoons \text{phenyl} \quad (627)$$

and

$$\text{i-}C_4H_3 + C_2H_3 \rightleftharpoons \text{phenyl} + H. \quad (628)$$

In their theoretical study, Madden *et al.*[72] also identified this n-C_4H_3 formation pathway on the potential energy surface of phenyl decomposition. The low-pressure rate constant for the forward reaction suggested by Westmoreland *et al.*[73] from a study of single-ring aromatics formation by chemically activated reactions was used in the present work. Reaction (628) was taken from Pope and Miller.[41] Recombination of phenyl with H to benzene, *i.e.*,

$$C_6H_5 + H \rightleftharpoons C_6H_6 \quad (634)$$

was found to be only a minor phenyl consumption pathway and that in all three rich flames investigated here. Depending on the local conditions, reaction (634) contributed at certain heights above the burner even to phenyl formation. Recombi-

nation of phenyl and hydrogen to benzene competes with hydrogen abstraction leading to benzyne and molecular hydrogen:

$$C_6H_5 + H \rightleftharpoons \text{benzyne} + H_2. \quad (635)$$

Low pressure rate constants determined for both channels by Mebel *et al.*[74] in an *ab initio* MO/RRKM study were used here. However, in all the flames studied here, reaction (635) was found not to contribute significantly to phenyl decomposition.

In the early part of the reaction zone, phenyl consumption occurred mainly by reaction with molecular oxygen,

$$C_6H_5 + O_2 \rightleftharpoons C_6H_5O + O. \quad (629)$$

The rate constant of this reaction is pressure-dependent particularly at higher temperatures. Kinetics for reaction (629) were determined by QRRK computations[55] using input parameters from the supporting information of DiNaro *et al.*[75] Formation of benzoquinone ($C_6H_4O_2$) + H *via* phenyl oxidation has been suggested from a shock tube study by Frank *et al.*[76] Tan and Frank[44] included this pathway in their reaction mechanism used for modeling benzene oxidation in the same benzene flame studied here and observed a substantial reduction of the phenyl overprediction reported by other authors.[42,43,49] However, relative to the experimental data, the maximum was ~2 mm closer to the burner. Frank *et al.*[76] assumed the major product to be *p*-benzoquinone rather than its *ortho* isomer due to less stress in a transition state with a 1,4-O_2 bridge. Chai and Pfefferle,[77] using on-line mass spectrometry to study benzene oxidation in a well-mixed reactor, detected trace amounts of 108 u species which they attributed to benzoquinones. The observation of no or only traces of benzoquinones in another experimental and kinetic modeling study of benzene oxidation led Alzueta *et al.*[78] to conclude that *o*-benzoquinone formation should be the most likely product channel. However, *p*-benzoquinone would be expected to build up to considerable concentrations because of its thermal stability.[79]

Similar to the suggestion of Alzueta *et al.*,[78]

$$C_6H_5 + O_2 \rightleftharpoons o\text{-}C_6H_4O_2 + H \quad (684)$$

was included in the model developed in the present work and was found to be the second most important phenyl consumption pathway in the early part of the reaction zone. Fast decay of *o*-benzoquinone to cylcopentadienone *via*

$$o\text{-}C_6H_4O_2 \rightleftharpoons C_5H_4O + CO \quad (687)$$

led to the prediction of concentrations consistent with experimental data on 108 u species, mass originally assigned to C_7H_8O,[27] but with a profile shifted by ~1.5 mm towards the burner. The only pathway in the present model leading to *p*-benzoquinone is reaction of atomic oxygen with phenoxy radicals,

$$C_6H_5O + O \rightleftharpoons p\text{-}C_6H_4O_2 + H. \quad (686)$$

This reaction and a corresponding pathway to *o*-benzoquinone,

$$C_6H_5O + O \rightleftharpoons o\text{-}C_6H_4O_2 + H \quad (685)$$

were suggested by Lin and Mebel[80] based on an *ab initio* MO study. *p*-Benzoquinone is more stable by about 4 kcal mol^{-1} than its *ortho*-isomer and its consumption was found to be significantly slower. The model prediction of *p*-benzoquinone gave a more than threefold higher peak concentration than that of its *ortho*-isomer in Flame IV.

The comparison between model predictions and experimental data for phenyl in the benzene flame, given in Fig. 12, shows excellent agreement with two independent experimental measurements.[27,46] However, details of phenyl depletion by reaction with molecular oxygen, particularly the relative contributions of pathways leading to phenoxy, *ortho*- and eventually *p*-benzoquinone at different pressures and temperatures, are not completely understood.

The analysis of phenyl formation in the rich acetylene and ethylene flames, Flames I and III, confirmed the above qualitative picture gained from Flame IV.

Phenol and phenoxy. The above discussion of benzene and phenyl consumption identifies phenoxy radical (C_6H_5O) as a major intermediate. Analysis of the contributions of individual reactions to C_6H_5O production showed reactions (629) and (646) to be dominant in the benzene flame. Unimolecular decay to cyclopentadienyl and CO *via*

$$C_6H_5O \rightleftharpoons C_5H_5 + CO \quad (668)$$

was found to be the major consumption pathway using the rate constant of Lin and Lin[81] from a shock tube study by covering pressure and temperature ranges of 0.4–0.9 atm and between 1000–1580 K. In the early part of the reaction zone, with a maximum reaction rate at ~5.5 mm from the burner, recombination of phenoxy with H to give phenol, *i.e.*,

$$C_6H_5O + H \rightleftharpoons C_6H_5OH, \quad (667)$$

contributes significantly to phenoxy consumption while the reverse reaction was found to be relatively unimportant in phenoxy formation between 7 and 11 mm.

Study of rates of production of phenol reveal reaction (667) to be the dominant formation pathway while, in agreement with the analysis of phenoxy formation and consumption, it contributes to phenol consumption in the later part of the reaction zone with a maximum reaction rate at ~8 mm from the burner. In this zone of the flame, reaction (652) was found to be the only significant phenol forming reaction. Besides hydrogen abstraction with OH,

$$C_6H_5OH + OH \rightleftharpoons C_6H_5O + H_2O, \quad (680)$$

unimolecular decomposition to cyclopentadiene (C_5H_6) and CO, *i.e.*,

$$C_6H_5OH \rightleftharpoons C_5H_6 + CO, \quad (671)$$

was the only important phenol consumption pathway identified. The rate constant deduced by Horn *et al.*[82] in a high-temperature shock tube experiment was used in the present work. Comparison in Fig. 14 of the model prediction with the experimental C_6H_5OH and C_5H_6 profiles in Flame IV is given and shows satisfactory agreement. The slight shift of the predicted

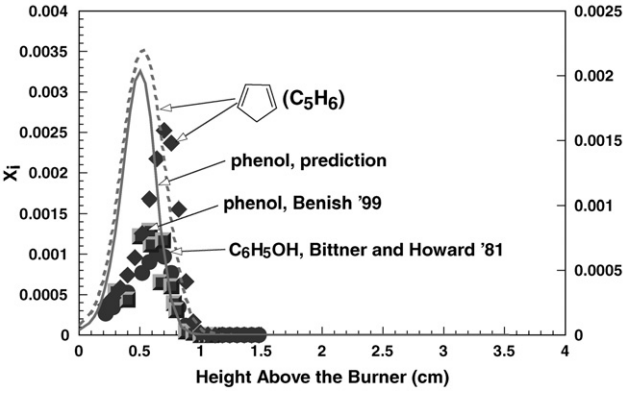

Fig. 14 Comparison between experimental mole fraction profiles and model predictions in a nearly sooting benzene/oxygen/argon flame (ϕ = 1.8, 30% argon, v = 50 cm s^{-1}, 20 Torr) C_6H_5OH: ● (experiment,[27] left scale); phenol: ■ (experiment,[46] left scale), — (prediction, left scale); C_5H_6: ◆ (experiment,[27] right scale), --- (prediction, right scale).

profiles towards the burner is consistent with that observed for phenyl (Fig. 12) and might be attributable to imperfections in the superposition of mole fraction profiles with the temperature profile used in the computation.

Despite the good reproduction by the model of major intermediates such as phenyl, phenol and cyclopentadiene, unresolved questions concerning phenoxy formation and consumption persist. No experimental phenoxy profile is available for the flames studied here but Hausmann *et al.*[45] measured a phenoxy profile with a peak mole fraction of 1.5×10^{-6} in a benzene flame under conditions, except for dilution concentration, identical to Flame IV. The model prediction of a phenoxy peak value exceeding 4×10^{-4} for Flame IV exceeds the Hausmann *et al.* value by more than two orders of magnitude which cannot be attributed to the dilution and associated temperature profile differences. In addition, a significant overprediction of phenoxy radicals was also reported by Shandross *et al.*[48] for a rich $H_2/O_2/Ar$ flame with benzene additive in which phenoxy concentration measured by MBMS was close to the detection limit.

Reasons for the phenoxy overprediction might be an inadequate description of its formation, for instance the oxidation of phenyl with O_2 and the competion with other product channels such as ring opening or the formation of benzoquinones. In recent years, several computational studies of potential energy surfaces of phenyl + O_2[83] and of the unimolecular decomposition of phenylperoxy (C_6H_5OO)[84] and phenoxy[85] have been conducted. At lower temperatures the formation of a dioxiranyl radical

with both O atoms bonded to the same carbon, followed by further decomposition was identified to be lowest energy pathway subsequent to the formation of the initital phenylperoxy adduct.[83] However, scission of the O–O bond to form phenoxy and O radicals was found to be favorable at temperatures relevant to the present work, and at temperatures greater than about 1200 K direct formation of phenoxy and O without passing through C_6H_5OO was suggested.[83] Benzoquinones were not identified in the investigation of potential energy surfaces of either phenyl + O_2[83] or unimolecular decomposition of phenylperoxy.[84] The formation of this species *via* phenyl oxidation therefore remains questionable, while phenoxy can be considered a major product of the phenyl + O_2 reaction. However, a detailed investigation of the pressure and temperature dependence of the rate constants describing different product channels will be necessary for a quantitative assessment.

The potential energy surface including transition states of thermal decomposition of phenoxy radicals was explored by means of *ab initio* calculations.[85] In qualitative agreement with Lin and Lin,[81] cyclopentadienyl and CO were identified as final products. Bimolecular reaction of phenoxy with oxygen radicals has been investigated thoroughly by Lin and Mebel[80] in an *ab initio* molecular orbital study and different pathways including formation of *o*- and *p*-benzoquinone, oxygen addition to a bridging position and to the terminal oxygen of the phenoxy radical with subsequent O_2 elimination have been identified. Lin and Mebel[80] also found a transition state allowing for the insertion of a bridging oxygen into a C–C bond forming the seven-membered ring structure $C_6O(H_5)O$ but concluded this pathway to be significantly less favorable than oxygen migration which yields a six-membered species with oxygen atoms located at two adjacent carbons. Lin and Mebel[80] did not consider subsequent decay of $C_6O(H_5)O$ to cyclopentadienyl and CO_2 as suggested by Carpenter[86] based on semiempirical PM3 computations but concluded that this pathway deserved future study. Some experimental evidence for formation of cyclopentadienyl and CO_2 *via* reaction between phenoxy and O radicals was found in a flow reactor study by Buth *et al.*[87] Mass spectrometric analysis of the reaction products subsequent to molecular beam sampling and electron impact ionization led to the detection of mass peaks assigned to *p*-benzoquinone ($C_6H_4O_2$), C_5H_5 and CO_2. However, as CO_2 was only a minor component, representing less than 15%, relative to $C_6H_4O_2$, Buth *et al.*[87] concluded benzoquinone formation to be the major pathway of $C_6H_5O + O$ while a minor reaction channel would lead to $C_5H_5 + CO_2$. Based on the overall rate constant for $C_6H_5O + O$ of $1.68 \pm 0.35 \times 10^{14}$ cm^3 mol^{-1} s^{-1} measured by Buth *et al.*[87] at room temperature and low pressure (1–5 mbar), Alzueta *et al.*[78] assigned rate constants of 8.5×10^{13} cm^3 mol^{-1} s^{-1} to both the formation of *o*- and *p*-benzoquinone (reactions (685) and (686)) and $k = 1.0 \times 10^{13}$ cm^3 mol^{-1} s^{-1} to

$$C_6H_5O + O \rightleftharpoons C_5H_5 + CO_2. \qquad (670)$$

The rate constants suggested by Alzueta *et al.*[78] are included in the reaction mechanism developed in the present study. The present analysis of the rates of production of phenoxy in the benzene flame showed the formation of *o*- and *p*-benzoquinone *via* reaction with O radicals (reactions (685) and (686)) to be minor and reaction (670) to be insignificant. Additional work is needed to attain adequate understanding of phenoxy formation and consumption chemistry.

Five-membered ring species: cyclopentadienyl, cyclopentadiene and cyclopentadienone

Five-membered ring species are important intermediates in the degradation of benzene, phenyl and their oxidation products, in particular of phenoxy radicals. Recombination of cyclopentadienyl radicals followed by rearrangement and hydrogen loss appears likely to play a significant role in naphthalene formation under certain conditions.[36,37,47,49,88,89] Pathways for the formation and consumption of cyclic and aliphatic C_5 species were analyzed in this study in the acetylene and benzene flames in which the corresponding experimental mole fraction profiles are available.

Cyclopentadienyl. The rates of production of cyclopentadienyl (C_5H_5) show unimolecular decomposition of phenoxy (reaction (668)) to be the dominant formation pathway in the benzene flame. The only other significant contribution to cyclopentadienyl formation in this flame results from hydrogen abstraction from cyclopentadiene:

$$C_5H_6 + H \rightleftharpoons C_5H_5 + H_2. \qquad (590)$$

Recombination with hydrogen atoms, *i.e.*,

$$C_5H_5 + H \rightleftharpoons C_5H_6, \qquad (573)$$

was identified as the major cyclopentadienyl depletion pathway in the first part of the reaction zone with a maximum consumption rate at about 6 mm from the burner. Closer to the end of the reaction zone, at about 8.5 mm, the reverse reaction becomes a minor cyclopentadienyl formation route.

Cyclopentadienyl oxidation to cyclopentadienone (C_5H_4O), *i.e.*,

$$C_5H_5 + O \rightleftharpoons C_5H_4O + H \qquad (581)$$

is a significant contribution to C_5H_5 depletion in the center of the reaction zone. The rate constant of reaction (581) was determined by means of bimolecular QRRK[55] using the input parameters given by Zhong and Bozzelli.[90] No pressure dependence of reaction (581) was observed. Unimolecular decomposition of cyclopentadienyl is its most important consumption pathway in the later part of reaction zone, particularly close to the region of maximum temperature, a finding which is con-

sistent with the high activation energy of more than 100 kcal mol^{-1} of

$$C_5H_5 \rightleftharpoons C_3H_3 + C_2H_2. \quad (574)$$

The potential energy surface of unimolecular cyclopentadienyl reactions, including 1,2-hydrogen atom migration, ring opening and decomposition, was studied thoroughly by Moskaleva and Lin[91] using *ab initio* MO calculations. Subsequently, they determined kinetic properties for the different reaction channels by means of multichannel RRKM theory for pressures of 100 Torr, 1 atm and 10 atm covering a temperature range from 1000 to 3000 K. Data given for 100 Torr are used in the present work. Assessment of cyclopentadienyl production rates identified hydrogen abstraction from cyclopentadienyl to give cyclopentatriene *via* reactions

$$C_5H_5 + H \rightleftharpoons C_5H_4 + H_2 \quad (562)$$

and

$$C_5H_5 + OH \rightleftharpoons C_5H_4 + H_2O \quad (563)$$

to be a minor cyclopentadienyl consumption route. Cyclopentatriene is found to isomerize subsequently to 1,2-pentadiene-4-yne ($CH_2CCHCCH$) (reaction (569)†). Also, hydrogen abstractions to give cyclopentatrienyl radicals (reactions (553)–(555)†) are included in the model.

In the acetylene flame, the reactions leading to cyclopentadienyl radicals are qualitatively similar to those in the benzene flame but differences in the relative contributions of some reactions are observed. For instance, hydrogen abstraction from cylopentadiene by H and OH (reactions (590) and (593)†) contributes more to cyclopentadienyl formation than does phenoxy decomposition (reaction (668)). Formation of naphthalene *via* recombination of cyclopentadienyl radicals followed by rearrangement and hydrogen loss[36,37,47,49,88,89] played a role in cyclopentadienyl consumption only in the benzene flame.

Comparison of predicted cyclopentadienyl mole fraction profiles with experimental ones showed an overprediction of ~3.5 fold in the benzene flame (Fig. 15) and an underprediction of ~2-fold in the acetylene flame (Fig. 16). Based on the work of Moskaleva and Lin,[91] rearrangement of cyclopentadienyl to the acyclic C_5H_5 species 2-penten-4-ynyl ($CH_2CHCHCCH$) was included in the mechanism but in both flames its predicted mole fraction was more than two orders of magnitude smaller than that of cyclopentadienyl. Mole fraction profiles are also available for C_5H_2, C_5H_3, C_5H_4 in the acetylene flame and for C_5H_3 in the benzene flame. Encouraging agreements with less than four-fold differences from

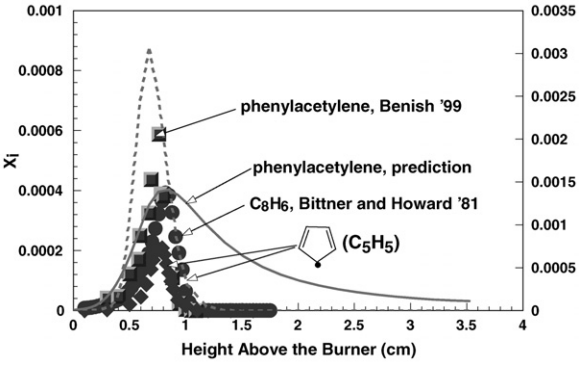

Fig. 15 Comparison between experimental mole fraction profiles and model predictions in a nearly sooting benzene/oxygen/argon flame ($\phi = 1.8$, 30% argon, $v = 50$ cm s^{-1}, 20 Torr); C_8H_6: ● (experiment,[27] left scale); phenylacetylene: ■ (experiment,[46] left scale), — (prediction, left scale); C_5H_5: ◆ (experiment,[27] right scale), --- (prediction, right scale).

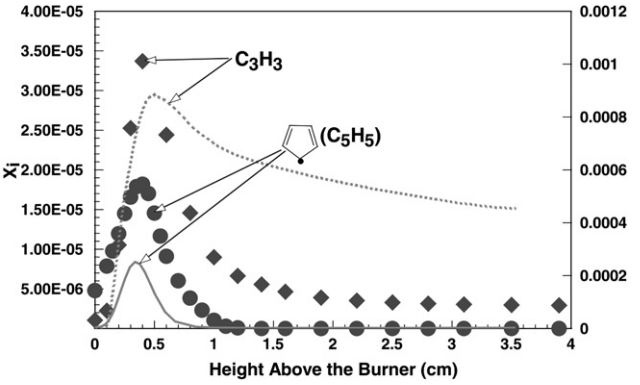

Fig. 16 Comparison between experimental mole fraction profiles[23,24] and model predictions in a fuel-rich acetylene/oxygen/argon flame ($\phi = 2.4$, 5% argon, $v = 50$ cm s^{-1}, 20 Torr); cyclopentadienyl (C_5H_5): ● (experiment, left scale), — (prediction, left scale); C_3H_3: ◆ (experiment, right scale), ··· (prediction, right scale).

experimental data were achieved for all of these species except C_5H_2 which is overpredicted by more than two orders of magnitude, probably due to the lack of consumption reactions. Cyclic and acyclic C_5H_4 and C_5H_3 species were included in the model but due to the nearly quantitative rearrangement of cyclopentatriene to 1,2-pentadiene-4-yne (reaction (569)†), predictions of the aliphatic species are significantly larger than those of their cyclic isomers. However, the current knowledge of thermodynamic and kinetic properties of C_5H_2, C_5H_3 and C_5H_4 species and the related chemistry is scarce and further developments might significantly effect the predicted relative concentrations of cyclic and aliphatic species.

Cyclopentadiene. Predicted cyclopentadiene mole fraction profiles generally compare satisfactorily to experimental data. However, a slight shift towards the burner in the benzene flame (Fig. 14) and a ~2-fold underprediction in the acetylene flame was observed. The net production rates of individual reactions contributing to cyclopentadiene formation and consumption indicate a close link to the cyclopentadienyl radical. Cyclopentadiene formation and consumption were found to occur much closer to the burner in the case of the acetylene flame with maxima and minima of the net production rate at about 0.8 mm and 2.5 mm compared to 6 mm and 8.5 mm in the benzene flame. In both flames but especially in the acetylene one, hydrogen addition to cyclopentadienyl, *i.e.*, reaction (573) is a major, and in first part of the reaction zone even dominant, formation pathway. The reverse direction of reaction (573) was studied experimentally by Roy *et al.*[92] Forward and reverse directions were expected to be significantly pressure-dependent, so the rate constant applied in the present work was determined by bimolecular QRRK calculation[55] using the input parameters given by Zhong and Bozzelli.[90] Unimolecular decay of phenol,[82] reaction (671), was found to be the major cyclopentadiene formation pathway in the later part of the reaction zone of the premixed benzene flame with a maximum net rate of reaction (671) at ~7 mm from the burner and also to play a significant role in the acetylene flame. Due to the importance of direct cyclopentadiene formation *via* reaction (671) in the later part of the reaction zone, reaction (573) contributes to cylopentadiene consumption at the end of the reaction zone of the benzene flame. Hydrogen abstraction from cyclopentadiene by H, OH and O to give cyclopentadienyl (reactions (590), (593) and (595)†) is the major C_5H_6 consumption route. The kinetic properties of the most important single reaction, reaction (590), were taken from Roy *et al.*[92] who studied the unimolecular decomposition of C_5H_6 behind reflected

shock waves. Bimolecular decomposition to give allyl (C_3H_5, H_2CCHCH_2) and C_2H_2, *i.e.*,

$$C_5H_6 + H \rightleftharpoons C_3H_5 + C_2H_2, \quad (592)$$

was identified as another major consumption pathway of C_5H_6, particularly in the benzene flame where its contribution was found to be as important as that of reaction (590). Reaction (592) was originally suggested by Dean,[93] and the rate constant given by Roy *et al.*[92] was used in the present work.

In addition to hydrogen-abstraction from the C-1 position of cyclopentadiene, *i.e.*, from a sp^3 carbon atom, hydrogen-abstraction from sp^2 carbon atoms by H, OH, O and CH_3 was included in the model (reactions (591), (594), (596) and (600)†) but was found to be only a negligible C_5H_6 consumption pathway due to the significantly higher C–H bond energy compared to that involving the sp^3 carbon atom.

Cyclopentadienone. The analysis of net rates of production of cyclopentadienone (C_5H_4O) showed unimolecular decomposition of o-benzoquinone, *i.e.*, reaction (687), suggested by Alzueta *et al.*,[78] and cyclopentadienyl oxidation *via* reaction (581), discussed above, to be the dominant formation pathways in both the acetylene and benzene flames. Other reaction sequences such as association to C_5H_5O,

$$C_5H_5 + O \rightleftharpoons C_5H_5O, \quad (579)$$

followed by hydrogen loss,

$$C_5H_5O \rightleftharpoons C_5H_4O + H, \quad (582)$$

suggested by Zhong and Bozzelli[90] and used by Alzueta *et al.*[78] have been implemented in the kinetic mechanism but did not contribute significantly to cyclopentadienone formation under the conditions investigated here. Reaction with H to give n-C_4H_5 and CO (reaction (587)†) was a major cyclopentadienone consumption pathway in both the acetylene and benzene flames while unimolecular decomposition to acetylene and CO,

$$C_5H_4O \rightleftharpoons 2C_2H_2 + CO, \quad (589)$$

played a significant role only in the benzene flame. Both pathways were included in the model of Alzueta *et al.*,[78] with parameters for the latter reaction based on a computational study of Wang and Brezinsky.[94] Wang and Brezinsky[94] explored the potential energy surface of thermal cyclopentadienone decomposition by means of *ab initio* MO calculations and subsequently determined kinetic parameters by RRKM theory for 0.1, 1, 10 and 100 atm. The potential energy surface showed isomerization to bicyclo-C_5H_4O

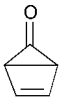

to be the inital step of cyclopentadienone decomposition, followed by formation of a CO-substituted four-membered ring species which decays to cyclobutadiene and CO. Similar to Alzueta *et al.*,[78] we assumed in the present work that cyclobutadiene readily dissociates to acetylene and used the Wang and Brezinsky[94] 0.1 atm kinetic parameters which are pertinent to the investigated conditions. Only reaction (589) was included in the final version of the mechanism (Table 3†). $C_5H_4O \rightleftharpoons$ bicyclo-C_5H_4O followed by bicyclo-$C_5H_4O \rightleftharpoons 2C_2H_2 + CO$ was found to be insignificant due to the potential energy of bicyclo-C_5H_4O which is 50.6 kcal mol^{-1} higher than that of C_5H_4O.[94] Another, minor, pathway of C_5H_4O consumption in the benzene flame is its oxidation to vinylacetylene and CO_2,

$$C_5H_4O + O \rightleftharpoons C_4H_4 + CO_2, \quad (588)$$

suggested by Alzueta *et al.*[78,79]

No unambiguous experimental identification of cyclopentadienone has been reported in the flames studied in this work. Comparison of the mole fraction profile measured by MBMS at 80 u in the benzene flame[27] with the cyclopentadienone profile predicted by the present kinetic model showed similar shape and peak location, but the predicted peak concentration is ~50-fold larger than the experimental value. Also, overlap with C_6H_8 species such as 1,3- and 1,4-cyclohexadiene, which have the same molecular mass as C_5H_4O cannot be excluded. There is clearly need for better understanding of formation and/or depletion of cyclopentadienone.

Benzene formation

Literature review. Qualitative and quantitative understanding of reaction pathways from aliphatic fuels to benzene and its derivatives is essential for an adequate description of fuel-rich combustion processes including formation of PAH and soot as mentioned earlier. In addition to one-ring aromatics, also species containing two rings, *e.g.*, naphthalene, can also be the first aromatic compound formed in a combustion environment. As mentioned above, recombination of cyclopentadienyl appears to form naphthalene.[36,37,47,49,88,89] However, cyclopentadienyl radicals are formed *via* phenoxy decomposition and hence are strongly linked to six-membered ring aromatics. Therefore, formation of naphthalene *via* cyclopentadienyl recombination is expected to be determined essentially by the efficiency of the formation of one-ring aromatic species, particularly benzene and phenyl.

Mainly two classes of pathways have been considered for the formation of one-ring aromatic species: (a) reactions of species containing four carbon atoms (C_4-species) with compounds containing two-carbon atoms (C_2-species) and (b) reactions between two molecules with three carbon atoms (C_3-species).

Cole *et al.*[95] computed rates of benzene production from mole fraction profiles determined by MBMS at different heights above the burner in a near-sooting premixed low pressure 1,3-butadiene flame. Based on kinetic data from the literature or from thermochemical estimations, Cole *et al.*[95] identified the reaction of the 1,3-butadienyl radical with acetylene followed by ring closure and hydrogen loss to be the dominant pathway leading to benzene under the conditions studied. Frenklach and Warnatz[34] suggested in a modeling study of a sooting low-pressure acetylene flame, cyclization of linear C_6H_5 (n-C_6H_5), the product of reaction between acetylene and n-C_4H_3, to be the dominant pathway at the higher flame temperatures. Both

$$n\text{-}C_4H_5 + C_2H_2 \rightleftharpoons C_6H_6 + H \quad (641)$$

and reaction (627) are included in the model developed in the present work. Westmoreland *et al.*[73] assessed benzene formation pathways in the same acetylene flame investigated in the present study.[23,24] They concluded that additions of n-C_4H_5 and n-C_4H_3 to acetylene would be sufficient to account for benzene formation in this flame and suggested the corresponding rate constants for different temperatures and pressures based on a bimolecular QRRK treatment for chemically activated reactions. A combined experimental/modeling study of a rich premixed low pressure acetylene flame led Bastin *et al.*[32] to conclude that $C_4H_5 + C_2H_2 \rightarrow$ benzene + H and $C_4H_3 + C_2H_2 \rightarrow$ phenyl can account for the formation of one-ring aromatic species. However, in the work of Bastin *et al.*[32] these reactions were treated as irreversible and n- and i-isomers of both C_4H_3 and C_4H_5 were lumped. Miller and Melius[33] re-examined the flame studied by Bastin *et al.*[32] and distinguished between n- and i-isomers for C_4H_3 and C_4H_5 in their model. They included isomerization between the corresponding isomers in their model with n-C_4H_3 and n-C_4H_5 being thermodynamically significantly less stable than their isomers. Based on the resulting model predictions, Miller

and Melius[33] concluded that reactions (641) and (627) were not sufficient to explain formation of the first aromatic ring in acetylene combustion under the conditions studied by Bastin *et al.*[32] even considering possible uncertainties in the thermodynamic or kinetic property data. Miller and Melius[33] investigated in some detail the possible contribution of propargyl (C_3H_3, H_2CCCH) recombination and of reaction of propargyl with C_3H_2 species and concluded that $C_3H_3 + C_3H_3 \rightleftharpoons C_6H_5 + H$ represents a potential pathway to one-aromatic ring species in acetylene flames. In the study of Miller and Melius,[33] the feasibility of this pathway was confirmed by means of the *ab initio* computational exploration of the potential energy surfaces between the different initial recombination products and benzene as well as phenyl + H. No prohibitive energy barrier was found for the subsequent isomerization steps. This conclusion is consistent with the work of Alkemade and Homann[96] who measured product distribution and the overall recombination rate constant in a temperature range of 623–673 K in a flow reactor operated at pressures between 300 and 600 kPa. The relative product yield of benzene was up to 30% while linear C_6H_6 species accounted for the remaining fraction. Recent modeling studies of premixed acetylene,[35] ethylene[36,37] and ethane[97] flames supported the dominant role of propargyl recombination in the formation of the first aromatic ring. Evidence of contributions of additional pathways, namely, vinyl addition to vinylacetylene[98] or 1,3-butadiene[99] was recently found in modeling of the premixed 1,3-butadiene flame of Cole *et al.*[95]

Despite complex sequences of rearrangement reactions identified by Miller and Melius[33] and suggested by Alkemade and Homann,[96] most authors describe the formation of phenyl *via* the global reaction $C_3H_3 + C_3H_3 \rightleftharpoons C_6H_5 + H$. However, Lindstedt and Skevis[35,98] included in their kinetic model elementary reaction steps forming different C_6H_6 isomers followed by isomerization to cyclic C_6H_6 species, *i.e.*, benzene and fulvene. Referring to master equation calculations, Pope and Miller[41] accounted for fulvene and phenyl + H as product channels of propargyl recombination with a nearly unity branching ratio. In addition, isomerization between fulvene and benzene was part of the reaction network they used for modeling premixed acetylene, ethylene and propene flames. The formation of fulvene as product of propargyl recombination is consistent the potential energy surface determined by Miller and Melius[33] but is in apparent contradiction with the experimental findings of Alkemade and Homann[96] as well as a recent high-temperature shock tube study of propargyl reactions under pyrolytic conditions[71] where detection of fulvene was not reported. However, in the pyrolysis of 1,5-hexadiyne, a product of propargyl recombination, conducted by Stein *et al.*[100] at atmospheric and very low ($<10^{-3}$ Torr) pressures, significant amounts of fulvene were identified, in particular at relative low temperatures and atmospheric pressure. A significant impact of the pressure was observed: at 1 atm, the fulvene/benzene ratio decreased steadily from 748 K to 833 K (the highest temperature reported for 1 atm) while at very low pressure fulvene and benzene were formed simultaneously, with a rate about 6 times faster for the latter species over the whole range of investigated temperatures, *i.e.*, up to 1073 K.

Benzene formation in acetylene and ethylene flames. In the present work, the rate constant used for reaction (638) is 3.0×10^{12} cm^3 mol^{-1} s^{-1}, consistent with several other studies.[36,37,97,98] The direct formation of benzene instead of phenyl + H is based on a pyrolytic shock tube study of propargyl reactions conducted by Scherer *et al.*[71] Pyrolytic reactions of propargyl radicals, produced by 3-iodo-propyne (C_3H_3I) decomposition, behind reflected shock waves were studied at 1000 to 1250 K. Residual gases were analyzed using gas chromatographic techniques (GC-FID and GC-MS) and atomic hydrogen was measured on-line by optical absorption. Formation of phenyl + H was found to represent less than 10% of the overall reaction rate.[71] Stable products comprised cyclic and linear C_6H_6 species and the product distribution shifted towards benzene in agreement with prior studies.[96,100]

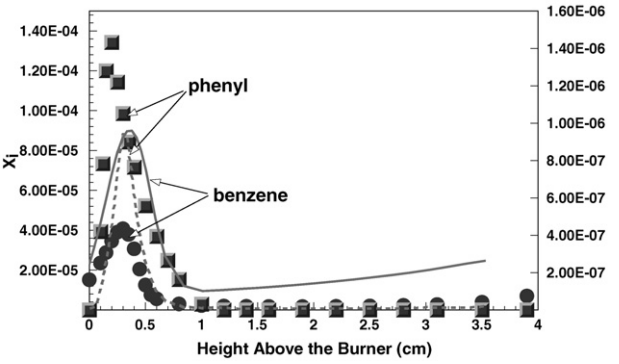

Fig. 17 Comparison between experimental mole fraction profiles[23,24] and model predictions in a fuel-rich acetylene/oxygen/argon flame ($\phi = 2.4$, 5% argon, $v = 50$ cm s^{-1}, 20 Torr); C_6H_6: ● (experiment, left scale), — (prediction, left scale); C_6H_5: ■ (experiment, right scale), --- (prediction, right scale).

Comparisons of model predictions for benzene and phenyl to experimental mole fraction profiles in the acetylene flame are given in Fig. 17. Benzene is by ~two-fold overpredicted while phenyl is underpredicted by ~40%. The experimentally observed increase of benzene in the postflame zone is overpredicted (Fig. 17), both the benzene and phenyl predictions in this zone are very sensitive to the temperature profile and the predicted benzene mole fraction in the postflame zone would attain values exceeding the maximum in the reaction zone if the originally published temperature profile[23,24] was used. A temperature drop of more than 300 K between 1.2 cm and 3.8 cm above the burner in the original profile is suspected to be at least partially induced by soot deposits on the thermocouple used. Therefore, the temperature profile was modified in the postflame zone (Fig. 1) for all model calculations of Flame I presented in this work.

The rates of production of benzene showed propargyl recombination (reaction (638)) to be the dominant benzene formation pathway in the acetylene flame. However, the net rate of this reaction shows its contribution to benzene depletion in the later part of the reaction zone with a maximum consumption rate at ~0.7 cm from the burner before again contributing to net benzene formation in the postflame zone. Close to the burner, a minor contribution to benzene production stems from reaction (652) with a maximum net rate at ~2 mm from the burner and with phenol formed by addition of H to phenoxy radicals (reaction (667)). Hydrogen abstraction, *i.e.*, reactions (644) and (647), was the major benzene consumption route in Flame I while the importance of phenoxy formation *via* reaction (646) was found to be secondary. The picture of phenyl formation and consumption is similar to that described above for the benzene flame. The major difference is the contribution of the isomerization of 1,3-dien-6-yne radicals and hydrogen addition to linear C_6H_4 (C_6H_4, 1,5-hexadiyn-3-ene), *i.e.*, the reverse of reactions (631) and (637), to phenyl formation close to burner before becoming consumption pathways beyond about 3.5 mm from the burner surface. The analysis of the rates of production showed that in Flame I, both linear C_6H_5 and C_6H_4 were formed sequentially from C_6H_2 (1,3,5-hexatriyne, triacetylene) resulting from reaction (613). Sequential growth of polyynes such as C_4H_2 and C_6H_2 was previously considered as a route to soot formation[7] but despite its minor contribution to phenyl formation close to the burner, no significant role of C_6H_2 in the formation of one-ring aromatics could be identified in the present work.

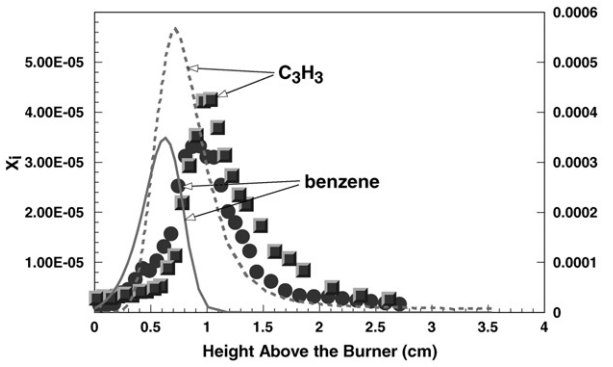

Fig. 18 Comparison between experimental mole fraction profiles[26] and model predictions in a fuel-rich ethylene/oxygen/argon flame ($\phi = 1.9$, 50.0% argon, $v = 62.5$ cm s^{-1}, 20 Torr); benzene: ● (experiment, left scale), — (prediction, left scale); C_3H_3: ■ (experiment, right scale), --- (prediction, right scale).

In the rich ethylene flame[26] (Flame III), the peak mole fraction of benzene is ~2-fold underpredicted and the computed profiles have a significantly narrower reaction zone than is found experimentally (Fig. 18). Propargyl recombination (reaction (638)) was identified as the dominant benzene formation pathway and the contribution of its reverse reaction to benzene consumption was found to be significantly more pronounced than in Flame I. As in Flame I, hydrogen abstraction by H and OH in reactions (644) and (647) was the other major benzene consumption route. Besides propargyl recombination, addition of vinyl to vinylacetylene, *i.e.*,

$$C_4H_4 + C_2H_3 \rightleftharpoons C_6H_6 + H, \qquad (639)$$

contributed to benzene formation in Flame III using the rate constant of Kubitza as cited by Lindstedt and Skevis.[98] Formation and consumption pathways of phenyl in Flame III are similar to those in Flame I, except for a contribution from reaction (628), suggested by Pope and Miller[41] and which is found to be a significant phenyl formation pathway in Flame III.

Reactions (641) and (627) are found to play no significant role in the formation of single-ring aromatics in both Flames I and III; the reverse of reaction (627) even contributes to phenyl depletion. However, meaningful assessment of relative contributions of different reactions requires adequate predictive capability for all involved species. Propargyl predictions satisfactorily agree with experimental C_3H_3 profiles in both Flames I and III and details of its formation and consumption are discussed below. The C_4H_3 and C_4H_5 isomers were undistinguishable with mass spectrometric analysis, so the MBMS measured mole fraction profiles represent the sum of n- plus i-C_4H_3 and n- plus i-C_4H_5. In the rich ethylene flame, the predicted i-C_4H_3 and i-C_4H_5 peak mole fractions are respectively ~20- and 75-fold than those of n-C_4H_3 and n-C_4H_5. Comparison of the sum of both isomers with the experimental profiles showed ~7- and 13-fold overpredictions for C_4H_3 and C_4H_5, respectively. The peak mole fraction of vinylacetylene (C_4H_4) was well predicted but the profile was shifted towards the burner by ~1 mm relative to the experimental profile.

In Flame I, shape and peak location of the computed vinylacetylene profile are in good agreement with experiment but the peak value is ~3-fold underpredicted. The sum of n- and i-C_4H_3 is ~3-fold overpredicted while the i-C_4H_3 was ~20-fold more abundant than n-C_4H_3. Unlike Flame III, the predicted mole fraction of n-C_4H_5 was only 4-fold smaller than that of i-C_4H_5 and the sum of both was ~10-fold underpredicted.

Under the conditions of the present work and using a given set of thermodynamic and kinetic property values, reaction (638) is found to be the dominant pathway leading to single-ring aromatics in the acetylene and ethylene flames. Addition of vinyl to vinylacetylene contributes to some extent in the ethylene combustion. However, because of remaining uncertainties, particularly the thermodynamic properties of C_4H_3 and C_4H_5 species, which might affect the relative abundances of the n- and i-isomers, the possibility of a significant contribution of n-C_4H_3 or n-C_4H_5 to phenyl and benzene formation cannot be definitively excluded. Also, additional work is required to achieve sufficient quantitative understanding of the formation of one-ring aromatic species *via* propargyl self-combination under different combustion conditions. A thorough analysis, *e.g.*, by means of a multi-well QRRK treatment,[55] will be necessary to determine pressure and temperature dependence of kinetics properties and product distributions.

In addition to reactions involving species containing two, three or four carbon atoms, five-membered ring species might also contribute to the formation of one-ring aromatic species. A reaction sequence beginning with cyclopentadienyl and methyl leading to fulvene and subsequently benzene has been suggested based on exploration of the corresponding potential energy surface by means of *ab initio* computations.[88,101] A benzene formation pathway beginning with the reaction between ethylene and cyclopentadiene has been also suggested.[38] Formation of one-ring aromatic species in pathways involving five-membered ring species have not been investigated in the present work, mostly due to the lack of available kinetics property data, but deserve attention in future work.

Propargyl, allene and propyne. Due to the importance of propargyl (H_2CCCH) for the formation of the first aromatic ring in the case of fuel-rich acetylene and ethylene combustion, its formation and consumption were studied in some detail. Thermodynamic property values of propargyl and related species such as C_3H_2, allene and propyne (Table 2†) were updated using *ab initio* computations on a CBS-Q level.[52,102] Its production rates show that, in both the acetylene and ethylene flames, formation and consumption of propargyl were closely connected to C_3H_2 as well as the two C_3H_4 isomers, allene (CH_2CCH_2) and propyne (methylacetylene, CH_3CCH). In agreement with Mebel *et al.*,[103] the structure HCCCH (propargylene) was assigned to the C_3H_2 species. With propargylene (HCCCH) as product, Mebel *et al.*[103] determined the bond dissociation energy of propargyl (CH_2CCH) to be 94.1 kcal mol^{-1} in comparison to 96.3 kcal mol^{-1} if vinylidenecarbene (H_2CCC) is formed. Similar to the results of Nguyen *et al.*,[104] the triplet electronic state was found to have the lowest energy[102] and was used in the present work. The heat of formation of 129.6 kcal mol^{-1}, used in the present work (Table 2†), is smaller by about 3 kcal mol^{-1} than that suggested by Nguyen *et al.*[104] Effects of potential uncertainties in thermodynamic property values are expected to be minimized by the consistency of the computational technique used for all C_3H_x species.

The rates of production of propargyl in the premixed acetylene flame showed H addition to C_3H_2 to be a major formation pathway while hydrogen abstraction *via*

$$C_3H_3 + H \rightleftharpoons C_3H_2 + H_2 \qquad (313)$$

was identified as the dominant propargyl consumption route. H addition to C_3H_2 is included in the model as the reverse of unimolecular dissociation of propargyl,

$$C_3H_3 \rightleftharpoons C_3H_2 + H. \qquad (312)$$

Unimolecular dissociation of propargyl was investigated theoretically by Mebel *et al.*[103] and the rate constant suggested by Scherer *et al.*[71] was used in the present work. Formation of C_3H_2 in the model occurs exclusively by hydrogen abstraction from propargyl by reaction with H and to some extent OH

radicals (reactions (313) and (314)†). The reverse of reaction (312) was found to be the most important C_3H_2 consumption reaction, consistent with its importance in propargyl formation. In addition, oxidation with OH and O, *i.e.*,

$$C_3H_2 + O \rightleftharpoons C_2H_2 + CO, \quad (309)$$

$$C_3H_2 + OH \rightleftharpoons C_2H_2 + HCO, \quad (310)$$

and

$$C_3H_2 + OH \rightleftharpoons CHCHCHO \quad (311)$$

contributed significantly to C_3H_2 depletion. Mole fraction profiles computed for C_3H_3 and C_3H_2 in Flame I are compared to experimental data in Fig. 16 and Fig. 19. Overprediction of both species in the postflame zone could indicate a need for additional consumption pathways. C_3H_2 formation and C_3H_3 consumption (and vice versa) are strongly coupled. Reaction (321), with $^1CH_2$, and particularly at the end of the reaction zone,

$$^3CH_2 + C_2H_2 \rightleftharpoons C_3H_3 + H \quad (322)$$

are major propargyl formation reactions. Based on the work of Böhland *et al.*,[105] reaction of $^3CH_2 + C_2H_2$ is assumed to yield directly propargyl and hydrogen atoms at the conditions pertinent to the present work. The rate constant determined by these authors is used here. Addition of $^1CH_2$ to C_2H_2 is expected to form chemically activated cyclopropene followed by isomerization to allene and propyne with subsequent hydrogen loss to give propargyl. In order to account for the pressure dependence of the $^1CH_2 + C_2H_2$ reaction, a QRRK analysis[55] was performed and the resulting rate constants are included in the model. The experimental rate constant of Böhland *et al.*[105] for the entrance channel was used while kinetics parameters for cyclopropene isomerization were taken from a combined experimental and computational study of Karni *et al.*[106] The isomerization allene ⇌ propyne was found to proceed in a series of successive reactions *via* cyclopropene,[106,107] so the direct reaction is not included. Kinetic parameters for unimolecular hydrogen loss from allene and propyne were taken from the shock tube study of Scherer *et al.*[71] The QRRK results reveal a significant pressure dependence of the relative contributions of the four product channels included, *i.e.*, cyclopropene, allene, propyne and propargyl + H. At pressures below 1 atm, propargyl + H is found to be the fastest pathway over the whole temperature range investigated, *i.e.*, from 300 to 2100 K.

In addition, hydrogen abstraction from allene and propyne by reaction with H and OH radicals, *i.e.*, reactions (379)–(382)†, contributed to some extent to propargyl formation. Hydrogen addition to propargyl, included as reverse reactions of unimolecular decomposition of allene and propyne (reactions (356) and (357)†), was found to play some role in propargyl depletion. Due to the use of mass spectrometric analysis, no experimental distinction between C_3H_4 isomers was possible. Model predictions for both allene and propyne are compared in Fig. 19 to the profile of the sum of all C_3H_4 species measured in Flame I. The predicted peak mole fraction of cyclopropene is $\sim 10^4$-fold smaller than those of allene and propyne. The reverse reactions of unimolecular decomposition of allene and propyne are major formation pathways of both species, particularly close to the burner. In the later part of the reaction zone, reactions

$$\text{allene} + H \rightleftharpoons C_2H_2 + CH_3 \quad (368)$$

$$CH_3 + C_2H_2 \rightleftharpoons \text{propyne} + H \quad (383)$$

and

$$\text{allene} + H \rightleftharpoons C_3H_5(\text{allyl}, H_2CCHCH_2), \quad (385)$$

are found to be major, even dominant, allene and propyne formation pathways while they contribute net depletion of these species close to the burner. Reaction

$$C_2H_3 + CH_3 \rightleftharpoons C_3H_5 + H \quad (395)$$

was identified to be mainly responsible for allyl (C_3H_5, H_2CCHCH_2) formation. Hydrogen abstraction reactions are the major allene and propyne depletion routes.

The comparison of the model predictions with experimental mole fraction profiles for C_3H_2, C_3H_3 and C_3H_4 species in the rich ethylene flame (Flame III) shows at least satisfactory agreement (Figs. 18 and 20). In contrast to the acetylene flame (Flame I), allene was predicted to be more abundant than propyne. Similar to Flame I, propargyl depletion occurs by hydrogen abstraction leading to C_3H_2 and oxidation with O and OH radicals which also consume C_3H_2 subsequently. Propargyl formation was found to be significantly different from that in Flame I. Reactions of $^1CH_2$ and $^3CH_2$ (reactions (321) and (322)) were only secondary pathways despite the good agreement of the predicted sum of these isomers with the experimental CH_2 profile. Hydrogen abstractions by H and OH from allene and propyne (reactions (379)–(382)†) are the dominant propargyl formation pathways. Unimolecular hydrogen loss from allene, reaction

$$\text{allene} \rightleftharpoons C_3H_3 + H, \quad (356)$$

is found to contribute to propargyl formation beyond ~6.5 mm from the burner while the reverse reaction is a minor propargyl consumption pathway in the first part of the reaction

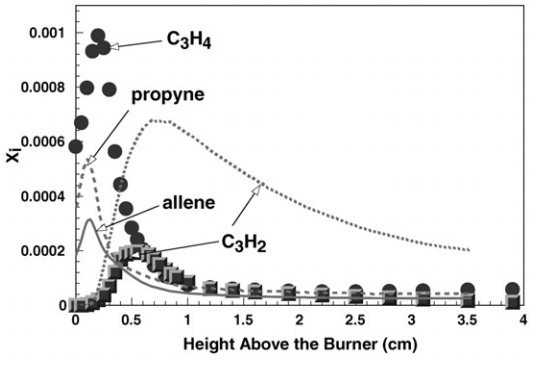

Fig. 19 Comparison between experimental mole fraction profiles[23,24] and model predictions in a fuel-rich acetylene/oxygen/argon flame ($\phi = 2.4$, 5% argon, $v = 50$ cm s^{-1}, 20 Torr); C_3H_4: ● (experiment); allene: — (prediction); propyne: --- (prediction); C_3H_2: ◆ (experiment), ··· (prediction).

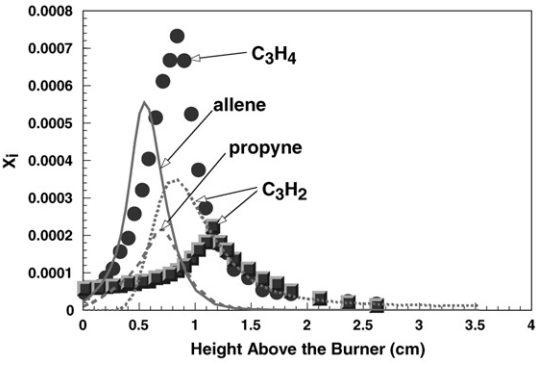

Fig. 20 Comparison between experimental mole fraction profiles[26] and model predictions in a fuel-rich ethylene/oxygen/argon flame ($\phi = 1.9$, 50.0% argon, $v = 62.5$ cm s^{-1}, 20 Torr); C_3H_4: ● (experiment); allene: — (prediction); propyne: --- (prediction); C_3H_2: ◆ (experiment), ··· (prediction).

zone. Major allene formation pathways are unimolecular propenyl decay, *i.e.*, the reverse of reaction (385) with allyl (C_3H_5, H_2CCHCH_2) formed by methyl addition to vinyl (reaction (395)), as well as

$$CH + C_2H_4 \rightleftharpoons C_3H_5. \quad (384)$$

The rate constant for reaction (384) was determined by a QRRK computation. Hydrogen abstractions (reactions (379) and (380)†) leading to propargyl contribute significantly to allene depletion, as do also acetylene and methyl formation *via* reaction (368) and isomerization to cyclopropene (reaction (362)†). Cyclopropene, predicted only in trace quantities, is found to isomerize nearly quantitatively to propyne (reaction (363)†), and this reaction is the dominant propyne formation pathway. Unimolecular decomposition of propyne to propargyl and H (reaction (357)†) contributes to its consumption beyond about 8 mm from the burner but is a propyne formation pathway closer to the burner. Finally, H addition leading to methyl and acetylene, the reverse of reaction (383), is found to be a major propyne consumption pathway.

Formation of PAH

Consumption of single-ring aromatics such as benzene and phenyl and also cyclopentadienyl plays important roles in molecular weight growth in fuel-rich combustion. Reaction pathways leading to PAH containing up to six condensed rings and C_{60} and C_{70} fullerenes in a benzene flame ($\phi = 2.4$)[50] were reported previously.[49] A detailed analysis of the formation of PAH with up to three aromatic rings in Flame IV[27,46] was published recently.[47] The data set of Benish[46] will be used for the further development of the reaction network presented in this work, particularly its extension to larger species. Benish[46] detected and quantified radical species up to 201 u and stable compounds up to 276 u using the nozzle beam sampling/radical scavenging method of Hausmann *et al.*[45] with subsequent analysis by GC-MS.

The reaction mechanism used in the present work (Table 3†) includes the formation of PAH with up to three condensed aromatic rings, *i.e.*, phenanthrene and anthracene. Although larger PAH are of general concern, in the flames studied here the concentrations of larger PAH not included in the model are small enough relative to the concentrations of PAH that are included, so that a significant part of the error that would be incurred by not including any PAH and their reactions with smaller species is avoided. The peak mole fraction of phenylacetylene, the largest species measured in the acetylene flame,[23,24] is ~3-fold overpredicted while good agreement of peak height and location is seen for both experimental profiles[27,46] in the benzene flame (Fig. 15). Kinetics parameters determined by transition state theory and taking into account chemical activation[51] are used in the description of phenylacetylene formation. Phenylacetylene mole fraction is overpredicted in the postflame zone in both the acetylene and benzene flames, possibly indicating the need to include additional consumption pathways as those involved in PAH and soot growth. Also, multiple-substituted phenylacetylene, *e.g.*, 1,2-, 1,3- or 1,4-diethynylbenzene, might be formed. Oxidation of phenylacetylene by O radicals to give phenylcarbene (C_6H_5CH), suggested by Eichholtz *et al.*[108] (reaction (740)†), and subsequent reactions leading to benzyl (reaction (741)†) and benzene (reactions (743) and (744)†) are included in the present model. Thermodynamic properties of triplet phenylcarbene were determined using the CBS-RAD *ab initio* computational procedure.[102,109] A heat of formation (ΔH_f°) of 110.6 kcal mol^{-1} was obtained.[102] Finally, oxidation of the phenylacetylene side chain by O radicals was found to have only a limited effect on phenylacetylene profiles in the postflame zone.

4. Conclusions

Kinetic modeling is becoming an increasingly valuable tool for combustion process optimization including minimization of pollutants present in the exhaust gas. The meaningful application of kinetic modeling requires sufficient predictive capability under a large range of conditions. Therefore, reaction mechanisms need to be critically tested against experimental data from well-defined and easy to model flames. Mole fraction profiles measured in unidimensional laminar premixed low-pressure flames using MBMS are well suited for use in the development and testing of kinetic models. Such data include not only reactants and products but also radical intermediates. The data on radicals allow particularly sensitive testing of the predictive capability of kinetic models. Premixed flames offer a large range of temperatures up to above 2000 K, pertinent to practical combustion devices and valuable for the assesssment of reaction mechanisms. Measured temperature profiles are part of the input necessary for modeling unidimensional premixed flames.

In the present work, published data on four premixed low pressure flames investigated by MBMS and thermocouple pyrometry were used for the development and testing of a reaction mechanism which describes the oxidation of the fuel as well as the formation of single-ring aromatics. The fuels studied are acetylene, ethylene, and benzene, thus including aliphatic and aromatic compounds pertinent to practical fuels. Responsive to the interest in the formation of PAH and soot in fuel-rich combustion, equivalence ratios of 2.4, 1.9 and 1.8 for ethylene, acetylene and benzene, respectively, were studied. In addition, a lean ($\phi = 0.75$) ethylene flame was investigated to assess the model under conditions of nearly complete fuel oxidation.

The kinetic model developed in the present work takes into account the recent literature. The thermodynamic and kinetic property databases were updated. In cases where reliable data were not available, density functional theory and in some case CBS-Q and CBS-RAD computations including vibrational analysis were conducted. QRRK analysis was used to determine pressure-dependent rate constants of chemically activated reactions.

Comparisons of model predictions with experimental mole fraction profiles show in all four flames the ability of the developed model to describe quantitatively the consumption of the fuel and oxygen and the formation of major oxidation products such as CO, CO_2 and water. H radical concentrations are overpredicted in the acetylene and lean ethylene flames while good agreement is achieved in the rich ethylene and in benzene flames. Excellent agreement of model predictions with experiment is observed for OH radicals, with a maximium deviation of ~40% overprediction in the lean ethylene flame. Discrepancies seen between experimental and computed mole fractions, particularly for radical species, might be related not only to imperfections of the model but also to uncertainties of the experimental temperature profile used as input for the model computations. Formation and consumption of methyl, the most abundant hydrocarbon radical, is reproduced correctly by the model but insufficient depletion of methane is observed in the postflame zone of the acetylene flame. Vinyl is ~3-fold underpredicted in the acetylene flame and up to 5-fold overpredicted in the rich ethylene and benzene flames. This finding might indicate some lack of quantitative understanding of the initial phase of acetylene and ethylene consumption, particularly the competition between addition and abstraction reactions with hydrogen atoms. Also, uncertainties on thermodynamic property data cannot be excluded.

In general, the predictive capability of the model is found to be at least satisfactory for most C_1, C_2, C_3 and C_4 hydrocarbons. However, C_4H_5 species are underpredicted in the acetylene flame. Propargyl recombination is found to be the

dominant benzene formation pathway in both acetylene and rich ethylene flames. The reaction between vinyl and vinylacetylene also contributes to benzene formation in ethylene combustion. A detailed investigation of the kinetics of propargyl self-combination including the temperature and pressure dependence of the different reaction products would be of much interest for future work. The ratio between n- and i-isomers of C_4H_3 and especially C_4H_5 might be affected by further improvements in thermodynamic property data; a change in the contribution of these species to benzene formation could result.

At least a qualitative understanding of benzene oxidation has been achieved. Benzoquinones are shown to be possible intermediates and their inclusion improved significantly the predictive capability of the model. However, the formation of benzoquinones by oxidation of phenyl remains questionable. In addition, the relative formation rates of *o*- and *p*-benzoquinone and possible additional consumption pathways of the latter isomer need to be addressed. Cyclopentadienyl radicals are found to be formed in all flames studied by unimolecular decay of phenoxy radicals. Unimolecular reaction to propargyl and acetylene and oxidation to cyclopentadienone are major cyclopentadienyl consumption pathways. A ~4-fold overprediction of cyclopentadienyl is observed in the benzene flame which might be related to uncertainties in phenoxy chemistry. Particularly, oxidation of phenyl by O_2 and the resulting product distribution at different temperatures and pressures need to be addressed in future work.

Finally, it can be concluded that at least satisfactory predictive capability has been found for ethylene, acetylene and benzene combustion at temperatures from near ambient up to nearly 2100 K. QRRK analysis is found to be suitable for estimating kinetics parameters of chemically activated reactions at specific pressures. An atmospheric pressure version of the present model is being developed and will be published later.

Acknowledgement

This research was supported by the Chemical Sciences, Geosciences and Biosciences Division, Office of Basic Energy Sciences, Office of Energy Research, U.S. Department of Energy under Grant DE-FGO2-84ER13282. We are grateful to Dr R. Sumathi for providing thermodynamic properties determined by CBS-Q and CBS-RAD computational techniques, Prof. W. H. Green and Dr O. Mazyar for contributions to the development of the thermodynamic and kinetic property data sets, and Prof. J. W. Bozzelli for providing software and valuable advice.

References

1 D. W. Dockery, C. A. Pope, X. Xu, J. D. Spengler, J. H. Ware, M. E. Fay, B. G. Ferris and F. E. Speizer, *N. Engl. J. Med.*, 1993, **329**, 1753–1759.
2 K. Siegmann and H. C. Siegmann, *Molecular Precursor of Soot and Quantification of the Associated Health Risk, Current Problems in Condensed Matter*, ed. Morán-López, Plenum Press, New York, 1998, pp. 143–160.
3 N. Künzli, R. Kaiser, S. Medina, M. Studnicka, O. Chanel, P. Filliger, M. Herry, F. Horak, Jr., V. Puybonnieux-Texier, P. Quénel, J. Schneider, R. Seethaler, J.-C. Vergnaud and H. Sommer, *Lancet*, 2000, **356**, 795–801.
4 F. J. Miller, D. E. Gardner, J. A. Graham, R. E. Lee, Jr., W. E. Wilson and J. D. Bachmann, *J. Air Pollut. Control Assoc.*, 1979, **29**, 610–615.
5 J. L. Durant, W. F. Busby, A. L. Lafleur, B. W. Penman and C. L. Crespi, *Mutat. Res.*, 1996, **371**, 123–157.
6 M. F. Denissenko, A. Pao, M.-S. Tang and G. P. Pfeifer, *Science*, 1996, **274**, 430–432.
7 B. S. Haynes and H. Gg. Wagner, *Prog. Energy Combust. Sci.*, 1981, **7**, 229–273.
8 H. Richter and J. B. Howard, *Prog. Energy Combust. Sci.*, 2000, **26**, 565–608.
9 J. O. Allen, N. M. Dookeran, K. A. Smith, A. F. Sarofim, K. Taghizadeh and A. L. Lafleur, *Environ. Sci. Technol.*, 1996, **30**, 1023–1031.
10 J.-B. Donnet, R. C. Bansal and M.-J. Wang, *Carbon Black: Science and Technology*, Dekker, New York, 2nd edn., 1993.
11 J. B. Howard, J. T. McKinnon, M. E. Johnson, Y. Makarovsy and A. L. Lafleur, *J. Phys. Chem.*, 1992, **96**, 6657–6662.
12 J. B. Howard, *Proc. Combust. Inst.*, 1992, **24**, 933–946.
13 J. B. Howard, A. L. Lafleur, Y. Makarovsky, S. Mitra, C. J. Pope and T. K. Yadav, *Carbon*, 1992, **30**, 1183–1201.
14 H. Richter, A. Fonseca, S. C. Emberson, J.-M. Gilles, J. B. Nagy, P. A. Thiry, R. Caudano and A. A. Lucas, *J. Chim. Phys.*, 1995, **92**, 1272–1285.
15 H. Richter, A. J. Labrocca, W. J. Grieco, K. Taghizadeh, A. L. Lafleur and J. B. Howard, *J. Phys. Chem. B*, 1997, **101**, 1556–1560.
16 J. B. Howard, K. D. Chowdhury and J. B. Vander Sande, *Nature*, 1994, **370**, 603.
17 K. D. Chowdhury, J. B. Howard and J. B. Vander Sande, *J. Mater. Res.*, 1996, **11**, 341–347.
18 H. Richter, K. Hernadi, R. Caudano, A. Fonseca, H.-N. Migeon, J. B. Nagy, S. Schneider, J. Vandooren and P. J. Van Tiggelen, *Carbon*, 1996, **34**, 427–429.
19 W. J. Grieco, J. B. Howard, L. C. Rainey and J. B. Vander Sande, *Carbon*, 2000, **38**, 597–614.
20 P. Hebgen, A. Goel, J. B. Howard, L. C. Rainey and J. B. Vander Sande, *Proc. Combust. Inst.*, 2000, **28**, 1397–1404.
21 R. L. Vander Wal and T. M. Ticich, *Chem. Phys. Lett.*, 2001, **336**, 24–32.
22 L. Yuan, K. Saito, W. Hu and Z. Chen, *Chem. Phys. Lett.*, 2001, **346**, 23–28.
23 P. R. Westmoreland, J. B. Howard and J. B. Longwell, *Proc. Combust. Inst.*, 1986, **21**, 773–782.
24 P. R. Westmoreland, PhD Thesis, Massachusetts Institute of Technology, Cambridge, MA, 1986.
25 A. Bhargava and P. R. Westmoreland, *Combust. Flame*, 1998, **115**, 456–467.
26 A. Bhargava and P. R. Westmoreland, *Combust. Flame*, 1998, **113**, 333–347.
27 J. D. Bittner and J. B. Howard, *Proc. Combust. Inst.*, 1981, **18**, 1105–1116.
28 H. Bockhorn, F. Fetting and H. W. Wenz, *Ber. Bunsen-Ges. Phys. Chem.*, 1983, **87**, 1067–1073.
29 M. Frenklach, D. W. Clary, W. C. Gardiner and S. E. Stein, *Proc. Combust. Inst.*, 1984, **20**, 887–901.
30 U. Bonne, K. H. Homann and H. Gg. Wagner, *Proc. Combust. Inst.*, 1965, **10**, 503–512.
31 P. Lindstedt, *Proc. Combust. Inst.*, 1998, **27**, 269–285.
32 E. Bastin, J.-L. Delfau, M. Reuillon, C. Vovelle and J. Warnatz, *Proc. Combust. Inst.*, 1981, **22**, 313–322.
33 J. A. Miller and C. F. Melius, *Combust. Flame*, 1992, **91**, 21–39.
34 M. Frenklach and J. Warnatz, *Combust. Sci. Technol.*, 1987, **51**, 265–283.
35 R. P. Lindstedt and G. Skevis, *Combust. Sci. Technol.*, 1997, **125**, 73–137.
36 M. J. Castaldi, N. M. Marinov, C. F. Melius, J. Huang, S. M. Senkan, W. J. Pitz and C. K. Westbrook, *Proc. Combust. Inst.*, 1996, **26**, 693–702.
37 A. D'Anna and A. Violi, *Proc. Combust. Inst.*, 1998, **27**, 425–433.
38 T. Faravelli, A. Goldaniga and E. Ranzi, *Proc. Combust. Inst.*, 1998, **27**, 1489–1495.
39 H. Wang and M. Frenklach, *Combust. Flame*, 1997, **110**, 173–221.
40 S. J. Harris, A. M. Weiner and R. J. Blint, *Combust. Flame*, 1988, **72**, 91–109.
41 C. J. Pope and J. A. Miller, *Proc. Combust. Inst.*, 2000, **28**, 1519–1527.
42 R. P. Lindstedt and G. Skevis, *Combust. Flame*, 1994, **99**, 551–561.
43 H.-Y. Zhang and J. T. McKinnon, *Combust. Sci. Technol.*, 1995, **107**, 261–300.
44 Y. Tan and P. Frank, *Proc. Combust. Inst.*, 1996, **26**, 677–684.
45 M. Hausmann, P. Hebgen and K.-H. Homann, *Proc. Combust. Inst.*, 1992, **24**, 793–801.
46 T. G. Benish, , PhD thesis, Massachusetts Institute of Technology, Cambridge, MA, 1999.

47 H. Richter, T. G. Benish, O. A. Mazyar, W. H. Green and J. B. Howard, *Proc. Combust. Inst.*, 2000, **28**, 2609–2618.
48 R. A. Shandross, J. P. Longwell and J. B. Howard, *Proc. Combust. Inst.*, 1996, **26**, 711–719.
49 H. Richter, W. J. Grieco and J. B. Howard, *Combust. Flame*, 1999, **119**, 1–22.
50 W. J. Grieco, A. L. Lafleur, K. C. Swallow, H. Richter, K. Taghizadeh and J. B. Howard, *Proc. Combust. Inst.*, 1998, **27**, 1669–1675.
51 H. Richter, O. Mazyar, R. Sumathy, W. H. Green, J. B. Howard and J. W. Bozzelli, *J. Phys. Chem. A*, 2001, **105**, 1561–1573.
52 R. Sumathi, H.-H. Carstensen and W. H. Green, *J. Phys. Chem. A*, 2001, **105**, 6910–6925.
53 http://web.mit.edu/richter/www/MITcomb.html.
54 A. M. Dean, J. W. Bozzelli and E. R. Ritter, *Combust. Sci. Technol.*, 1991, **80**, 63–85.
55 A. Y. Chang, J. W. Bozzelli and A. M. Dean, *Z. Phys. Chem.*, 2000, **214**, 1533–1568.
56 R. J. Kee, J. F. Grcar, M. D. Smooke and J. A. Miller, *A FORTRAN Program for Modeling Steady Laminar One-Dimensional Premixed Flames*, Sandia Report SAND85-8240, 1985.
57 R. J. Kee, F. M. Rupley and J. A. Miller, *Chemkin-II: A Fortran Chemical Kinetics Package for the Analysis of Gas-Phase Chemical Kinetics*, Sandia Report SAND89-8009, Sandia National Laboratory, Livermore, CA, 1989.
58 R. J. Kee, F. M. Rupley, J. A. Miller, M. E. Coltrin, J. F. Grcar, E. Meeks, H. K. Moffat, A. E. Lutz, G. Dixon-Lewis, M. D. Smooke, J. Warnatz, G. H. Evans, R. S. Larson, R. E. Mitchell, L. R. Petzold, W. C. Reynolds, M. Caracotsios, W. E. Stewart, P. Glarborg, C. Wang and O. Adigun, *CHEMKIN Collection*, Release 3.6, Reaction Design, Inc., San Diego, CA, 2000.
59 A. Burcat and B. McBride, 1997 Ideal Gas Thermodynamic Data for Combustion and Air-Pollution Use, Technion Aerospace Engineering (TAE) Report # 804 June 1997, ftp://ftp.technion.ac.il/pub/supported/aetdd/thermodynamics/.
60 NIST Chemistry WebBook, NIST Standard Reference Database Number 69, February 2000, ed. W. G. Mallard and P. J. Linstrom, National Institute of Standards and Technology, Gaithersburg, MD 20899, http://webbook.nist.gov/.
61 R. J. Kee, F. M. Rupley and J. A. Miller, *The Chemkin Thermodynamic Data Base*, Sandia Technical Report SAND87-8215B, UC-4, Sandia National Laboratories, Livermore, CA, April 1994.
62 W. Tsang and R. F. Hampson, *J. Phys. Chem. Ref. Data*, 1986, **15**, 1087.
63 V. D. Knyazev, Á. Bencsura, S. I. Stoliarov and I. R. Slagle, *J. Phys. Chem.*, 1996, **100**, 11346–11354.
64 H. Thiesemann, E. P. Clifford, C. A. Taatjes and S. J. Klippenstein, *J. Phys. Chem. A*, 2001, **105**, 5393–5401.
65 W. Tsang and J. A. Walker, *J. Phys. Chem.*, 1992, **96**, 8378–8384.
66 V. D. Knyazev and I. R. Slagle, *J. Phys. Chem.*, 1996, **100**, 16899–16911.
67 S. Madronich and W. Felder, *J. Phys. Chem.*, 1985, **89**, 3556–3561.
68 T. Ko, G. Y. Adusei and A. Fontijn, *J. Phys. Chem.*, 1991, **95**, 8745–8748.
69 A. M. Mebel, M. C. Lin, T. Yu and K. Morokuma, *J. Phys. Chem. A*, 1997, **101**, 3189–3196.
70 J. H. Kiefer, L. J. Mizerka, M. R. Patel and H.-C. Wei, *J. Phys. Chem.*, 1985, **89**, 2013–2019.
71 S. Scherer, T. Just and P. Frank, *Proc. Combust. Inst.*, 2000, **28**, 1511–1518.
72 L. K. Madden, L. V. Moskaleva, S. Kristyan and M. C. Lin, *J. Phys. Chem. A*, 1997, **101**, 6790–6797.
73 P. R. Westmoreland, A. M. Dean, J. B. Howard and J. P. Longwell, *J. Phys. Chem.*, 1989, **93**, 8171–8180.
74 A. M. Mebel, M. C. Lin, D. Chakraborty, J. Park, S. H. Lin and Y. T. Lee, *J. Chem. Phys.*, 2001, **114**, 8421–8435.
75 J. L. DiNaro, J. B. Howard, W. H. Green, J. W. Tester and J. W. Bozzelli, *J. Phys. Chem. A*, 2000, **104**, 10576–10586.
76 P. Frank, J. Herzler, T. Just and C. Wahl, *Proc. Combust. Inst.*, 1994, **25**, 833–840.
77 Y. Chai and L. D. Pfefferle, *Fuel*, 1998, **77**, 313–320.
78 M. U. Alzueta, P. Glarborg and K. Dam-Johansen, *Int. J. Chem. Kinet.*, 2000, **32**, 498–522.
79 M. U. Alzueta, M. Oliva and P. Glarborg, *Int. J. Chem. Kinet.*, 1998, **30**, 683–697.
80 M. C. Lin and A. M. Mebel, *J. Phys. Org. Chem.*, 1995, **8**, 407–420.
81 C.-Y. Lin and M. C. Lin, *J. Phys. Chem.*, 1986, **90**, 425–431.
82 C. Horn, K. Roy, P. Frank and T. Just, *Proc. Combust. Inst.*, 1998, **27**, 321–328.
83 C. Barckholtz, M. J. Fadden and C. M. Hadad, *J. Phys. Chem. A*, 1999, **103**, 8108–8117.
84 M. J. Fadden, C. Barckholtz and C. M. Hadad, *J. Phys. Chem. A*, 2000, **104**, 3004–8011.
85 S. Olivella, A. Solé and A. García-Raso, *J. Phys. Chem.*, 1995, **99**, 10549–10556.
86 B. K. Carpenter, *J. Am. Chem. Soc.*, 1993, **115**, 9806–9807.
87 R. Buth, K. Hoyermann and J. Seeba, *Proc. Combust. Inst.*, 1994, **25**, 841–849.
88 C. F. Melius, M. E. Colvin, N. M. Marinov, W. J. Pitz and S. M. Senkan, *Proc. Combust. Inst.*, 1996, **26**, 685–692.
89 J. Filley and J. T. McKinnon, *Combust. Flame*, 2001, **124**, 721–723.
90 X. Zhong and J. W. Bozzelli, *J. Phys. Chem. A*, 1998, **102**, 3537–3555.
91 L. V. Moskaleva and M. C. Lin, *J. Comput. Chem.*, 2000, **21**, 415–425.
92 K. Roy, C. Horn, P. Frank, V. G. Slutsky and T. Just, *Proc. Combust. Inst.*, 1998, **27**, 329–336.
93 A. M. Dean, *J. Phys. Chem.*, 1990, **94**, 1432–1439.
94 H. Wang and K. Brezinsky, *J. Phys. Chem. A*, 1998, **102**, 1530–1541.
95 J. A. Cole, J. D. Bittner, J. P. Longwell and J. B. Howard, *Combust. Flame*, 1984, **56**, 51–70.
96 U. Alkemade and K. H. Homann, *Z. Phys. Chem., Neue Folge*, 1989, **161**, 19–34.
97 N. M. Marinov, W. J. Pitz, C. K. Westbrook, M. J. Castaldi and S. M. Senkan, *Combust. Sci. Technol.*, 1996, **116-117**, 211–287.
98 R. P. Lindstedt and G. Skevis, *Proc. Combust. Inst.*, 1996, **26**, 703–709.
99 A. Goldaniga, T. Faravelli and E. Ranzi, *Combust. Flame*, 2000, **122**, 350–358.
100 S. E. Stein, J. A. Walker, M. M. Suryan and A. Fahr, *Proc. Combust. Inst.*, 1990, **23**, 85–90.
101 L. V. Moskaleva, A. M. Mebel and M. C. Lin, *Proc. Combust. Inst.*, 1996, **26**, 521–526.
102 R. Sumathi, personal communication, Massachusetts Institute of Technology, Cambridge, MA, 2001.
103 A. M. Mebel, W. M. Jackson, A. H. H. Chang and S. H. Lin, *J. Am. Chem. Soc.*, 1998, **120**, 5751–5763.
104 T. L. Nguyen, A. M. Mebel and R. I. Kaiser, *J. Phys. Chem. A*, 2001, **105**, 3284–3299.
105 T. Böhland, F. Temps and H. Gg. Wagner, *Proc. Combust. Inst.*, 1986, **21**, 841–850.
106 M. Karni, I. Oref, S. Barzilai-Gilboa and A. Lifshitz, *J. Phys. Chem.*, 1988, **92**, 6924–6929.
107 T. Kakumoto, T. Ushirogouchi, K. Saito and A. Imamura, *J. Phys. Chem.*, 1987, **91**, 183–189.
108 M. Eichholtz, A. Schneider, D.-V. Stucken, J.-T. Vollmer and H. Gg. Wagner, *Proc. Combust. Inst.*, 1994, **25**, 859–866.
109 P. M. Mayer, C. J. Parkinson, D. M. Smith and L. Radom, *J. Chem. Phys.*, 1998, **108**, 604–615.